Taxonomy of Maastrichtian–Thanetian Deep-Sea Ostracodes from U1407, IODP Exp 342, off Newfoundland, Northwestern Atlantic, part 2: Families Eucytheridae, Krithidae, Thaerocytheridae, Trachyleberididae, and Xestoleberididae

Authors: Yamaguchi, Tatsuhiko, Matsui, Hiroki, and Nishi, Hiroshi

Source: Paleontological Research, 21(2) : 97-121

Published By: The Palaeontological Society of Japan

URL: https://doi.org/10.2517/2016PR011

Paleontological Research, vol. 21, no. 2, pp. 97–121, April 1, 2017

doi:10.2517/2016PR011

Taxonomy of Maastrichtian–Thanetian deep-sea ostracodes from U1407, IODP Exp 342, off Newfoundland, Northwestern Atlantic, part 2: Families Eucytheridae, Krithidae, Thaerocytheridae, Trachyleberididae, and Xestoleberididae

TATSUHIKO YAMAGUCHI[1], HIROKI MATSUI[2] AND HIROSHI NISHI[3]

[1]*Center for Advanced Marine Core Research, Kochi University, B200 Monobe, Nankoku, Kochi 783-8502, Japan (e-mail: tyamaguchi@kochi-u.ac.jp)*
[2]*Department of Earth Science, Tohoku University, 6-3 Aramaki, Aoba, Aoba-ku, Sendai 980-8578, Japan*
[3]*Tohoku University Museum, Tohoku University, 6-3 Aramaki, Aoba, Aoba-ku, Sendai 980-8578, Japan*

Received September 8, 2015; Revised manuscript accepted April 1, 2016

Abstract. Little is known about the taxonomy of Paleocene ostracodes from ocean drilling sites. Herein, we report 14 ostracode species of the families Eucytheridae, Krithidae, Thaerocytheridae, Trachyleberididae, and Xestoleberididae from Cretaceous–Paleocene sediments at U1407 of Integrated Ocean Drilling Program Expedition 342 off Newfoundland, Northwestern Atlantic. We describe five trachyleberidid species new to science: *Croninocythereis clavae* sp. nov., *Phacorhabdotus flabellicarinus* sp. nov., *Poseidonamicus norrisi* sp. nov., *Ryugucivis blumi* sp. nov., and *Trachyleberidea cronini* sp. nov.

Key words: Cretaceous, Integrated Ocean Drilling Program Expedition 342, North Atlantic, Ostracoda, Paleocene

Introduction

To understand the deep-sea ecosystem and its evolution, taxonomic data are very important (e.g. Brökeland and George, 2009). The taxonomic data of deep-sea ostracodes contribute to discussion of biodiversity in response to climate changes and support inferences about the phylogeny of deep-sea ostracodes (e.g. Hunt, 2007; Yasuhara *et al*., 2009a). The taxonomy of Paleocene deep-sea ostracodes is poorly investigated. We already reported and described systematically 18 Paleocene ostracode species of the families Cytherellidae, Bairdiidae, Pontocyprididae, Bythocytheridae, and Cytheruridae from the Integrated Ocean Drilling Program (IODP) Expedition (Exp) 342 Site U1407 (Yamaguchi *et al*., 2017). Furthering that work, we have studied the taxonomy of the families Eucytheridae, Krithidae, Thaerocytheridae, Trachyleberididae, and Xestoleberididae at the site and describe herein five species new to science.

Material and methods

At Site U1407 (41°25’30”N, 49°48’28.8”W), three holes were drilled on the seafloor of the Southeast Newfoundland Ridge at 3073 m depth (Expedition 342 Scientists, 2012; Norris *et al*., 2014; Figure 1). We took 32 sediment samples of 10–40 cm^3 volume from the interval of 146.47–216.72 mcd in working half cores of Core 21X–22X of Hole A, Core 19X of Hole B, and Core 14X–18X and 20X of Hole C (Figure 2). A sample identifier for an IODP sample includes the following in order: Expedition (or Leg), Site, Hole, Core, Core type, Section, Section half, and Interval (cm). For example, a sample identifier expressed as 342-U1407A-22X-1W, 20–22 indicates Interval 20–22 cm of Section 1 in the working half of Core 22X of Hole A at Site U1407 of IODP Exp 342. “X” means a core that was collected using the extended core barrel. All the core sediments constitute nannofossil chalks with radiolarians at 146 to ~205 mcd and nannofossil chalks at ~205 to 221 mcd, showing pink to white in color. Using the planktic biostratigraphy, the

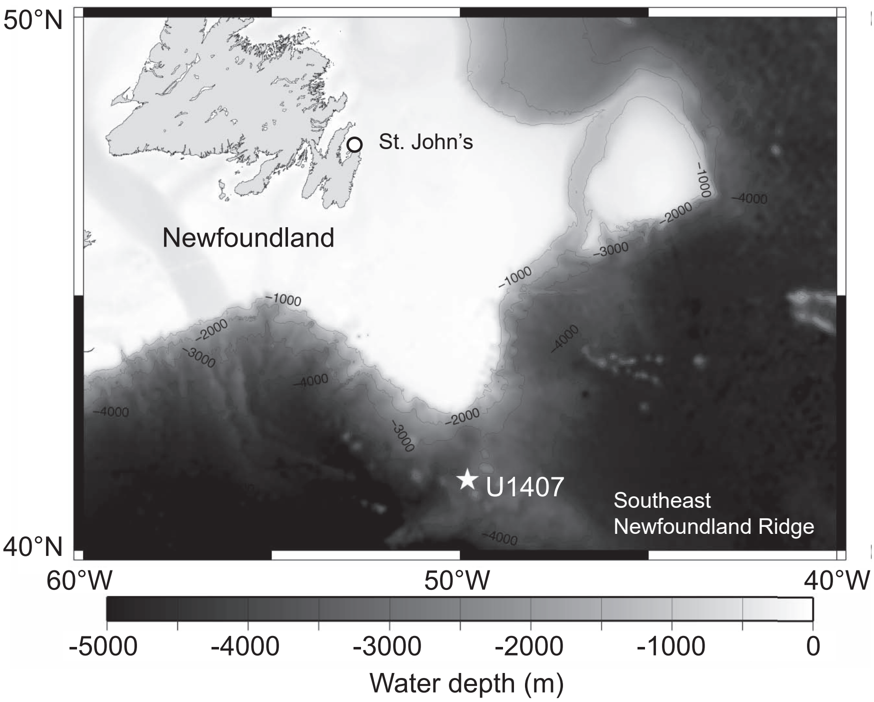

Figure 1. Location of the study site. Contours with numbers signify water depth in meters.

core sediments are dated to be ~66.3–57.4 Ma (the uppermost Maastrichtian to the Thanetian) (Norris *et al*., 2014; Figure 2).

For extracting ostracode specimens, we washed samples in tap water using a sieve of 32 µm opening. Then ostracode specimens were picked up from fractions of >150 µm, using a fine brush under a binocular microscope. The specimens were observed and their photos were taken with a scanning electron microscope (SEM) JSM-6500F (JEOL Ltd.) (Figures 3–8) and an optical microscope in order to identify them at species level and describe their morphological characters.

For illustrating the internal structures of the new species, the specimens were immersed in tap water in a Petri dish and observed under transmitted light with a digital microscope, VHX-2000 (Keyence, Ltd.). Images of the internal structures were also captured. Using the focus stacking system the digital microscope is equipped with, deep-focus images of the internal structures were made (Figures 9, 10). To identify shapes of marginal pore canals, vestibulum, and reticulation, characters were drawn on the images using Adobe Photoshop software (Figures 11–13). The specimens were measured using the digital microscope (Figure 14; Table 1). The scanning electron and digital microscopes are hosted at the Center for Advanced Marine Core Research, Kochi University.

For the systematic description, the general terminology and classification of taxonomic ranks higher than the genus broadly followed Horne *et al*. (2002). The general terminology for ostracode morphology followed Sylvester-Bradley and Benson (1971) and Horne *et al*. (2002). The terminology for *Abyssocythere* and *Herrigocythere*, for *Krithe*, and for *Poseidonamicus* morphologies were referred to Benson (1971), Coles *et al*. (1994), and Hunt (2007), respectively. The higher taxonomic ranks follow Brandão *et al*. (2016). The classification of carapace size according to Athersuch *et al.* (1989) is as follows: small (< 500 µm long); medium (500–650 µm long); large (> 650 µm long).

Podocopid ostracodes manifest sexual dimorphism in size and shape of their valves. Generally a male valve has a more slender shape than a female's (e.g. Horne *et al*., 2002; Ozawa, 2013). A male's valve shows a higher proportion of valve length (L) to height (H) than the female form's. We measured L and H of 17 adult specimens of *Poseidonamicus norrisi* sp. nov. and of 25 adult specimens of *Trachyleberidea cronini* sp. nov., calculated $(L-H)/L$ ratios, and graphed the frequency of the ratios as a histogram with kernel density estimation. When sexual dimorphism appears in $(L-H)/L$ ratios, the frequency and the kernel density estimation indicate a bimodal distribution. For the kernel density estimation, the Gaussian kernel was selected and the smoothing bandwidth was set according to "Silverman's rule of thumb" (Silverman,

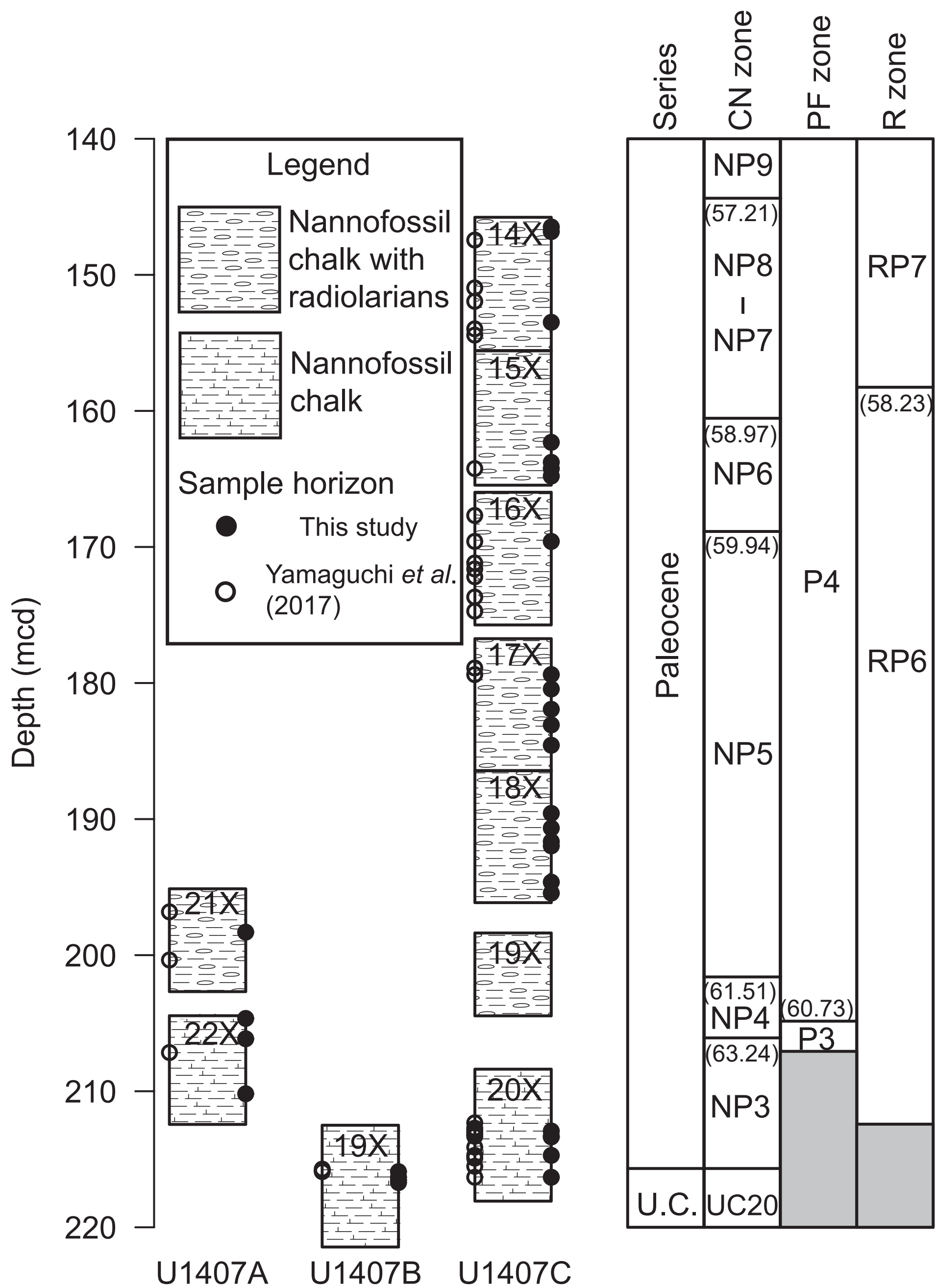

Figure 2. Lithostratigraphy and stratigraphic position of the examined samples. The biostratigraphic zones are referred to Martini (1971) and Burnett (1998) for calcareous nannofossils (CN), Wade *et al*. (2011) for planktic foraminifers (PF), and Sanfilippo and Nigrini (1998) for radiolarians (R). Numerals within parenthesis near the biostratigraphic zonal boundaries indicate the geological ages of the boundaries, following Gradstein *et al*. (2012). There is a hiatus between the top of the Cretaceous and the base of the Paleocene. The recovered cores, lithostratigraphy, and biostratigraphy are sourced from Norris *et al*. (2014). Abbreviation: U. C. = Upper Cretaceous.

1986). The density estimation was calculated and drawn using R software (R Core Team, 2015).

All the specimens from Site U1407 are registered and deposited in the National Museum of Nature and Science, Tsukuba (NMNS) and Scripps Institution of Oceanography (SIO), University of California, San Diego, which are the Microfossil Reference Centers for the International Ocean Discovery Program. The registered numbers at NMNS

Figure 3. SEM images of ostracode species. **A, B,** *Eucythere* sp. (MPC-29107); A, external view of adult LV; B, internal view of adult LV; **C, D,** *Krithe crassicaudata* Bold, 1946 (SIO-BIC-C12181); C, external view of adult LV; D, internal view of adult LV; **E, F,** *Krithe dolichodeira* Bold, 1946 s.l. (MPC-29112); E, external view of adult RV; F, internal view of adult RV; **G, H,** *Krithe* sp. (MPC-29113); G, external view of adult RV; H, internal view of adult RV. All scale bars indicate 100 μm.

and SIO have the prefixes of MPC and SIO-BIC, respectively. To describe *Poseidonamicus norrisi* sp. nov. and *Trachyleberidea cronini* sp. nov., we examined 27 specimens of the new species from Deep Sea Drilling Project (DSDP) Site 401, North Atlantic. The specimens were already investigated by Yamaguchi and Norris (2012)

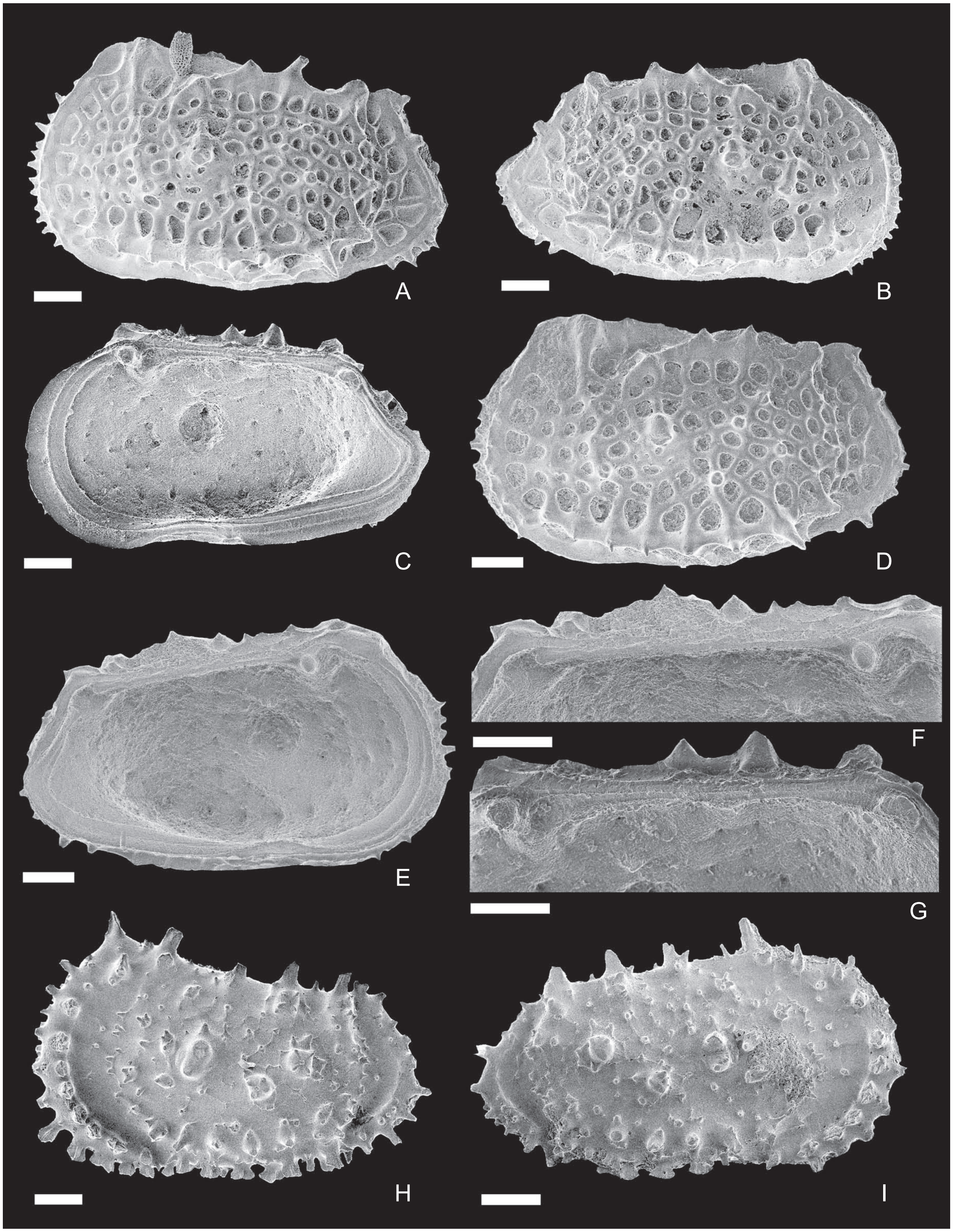

Figure 4. SEM images of ostracode species. **A–G,** *Poseidonamicus norrisi* sp. nov.; A, external view of adult LV (SIO-BIC-C12162, paratype); B, external view of adult male RV (MPC-29119, holotype); C, internal view of adult male RV (MPC-29119, holotype); D, external view of adult female LV (MPC-29120, paratype); E, internal view of adult female LV (MPC-29120, paratype); F, hingement of adult female LV (MPC-29120, paratype); G, hingement of adult male RV (MPC-29119, holotype); **H, I,** *Croninocythereis clavae* sp. nov.; H, external view of adult LV (MPC-29114, holotype); I, external view of adult RV (SIO-BIC-C12168, paratype). All scale bars indicate 100 μm.

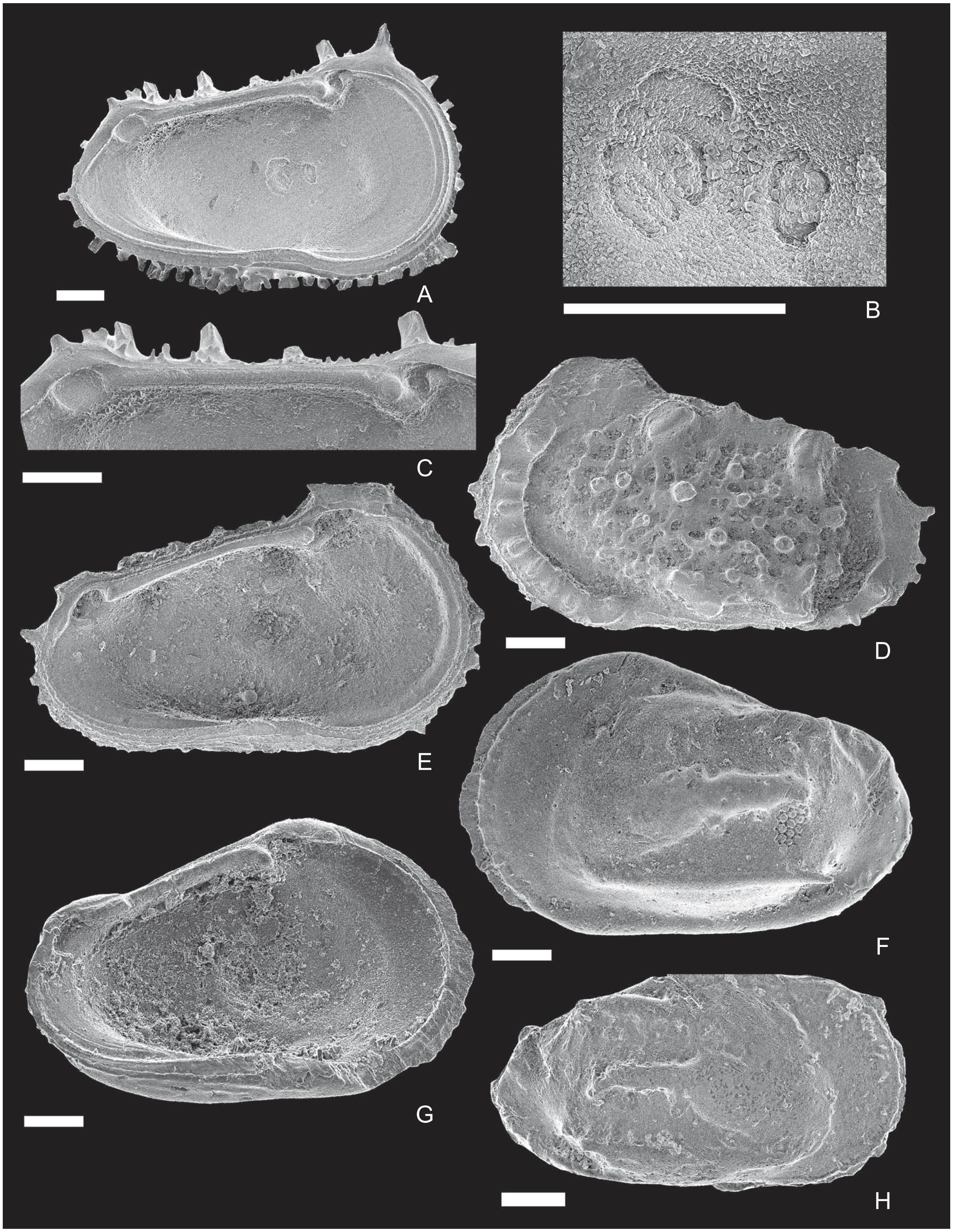

Figure 5. SEM images of ostracode species. **A–C,** *Croninocythereis clavae* sp. nov. (MPC-29114, holotype); A, internal view of adult LV; B, muscle scars of adult LV; C, hingement of adult LV; **D, E,** *Herrigocythere* sp. (MPC-29105); D, external view of adult LV; E, internal view of adult LV; **F–H,** *Phacorhabdotus flabellicarinus* sp. nov.; F, external view of adult LV (MPC-29116, holotype); G, internal view of adult LV (MPC-29116, holotype); H, external view of adult RV (SIO-BIC-C12187, paratype). All scale bars indicate 100 μm.

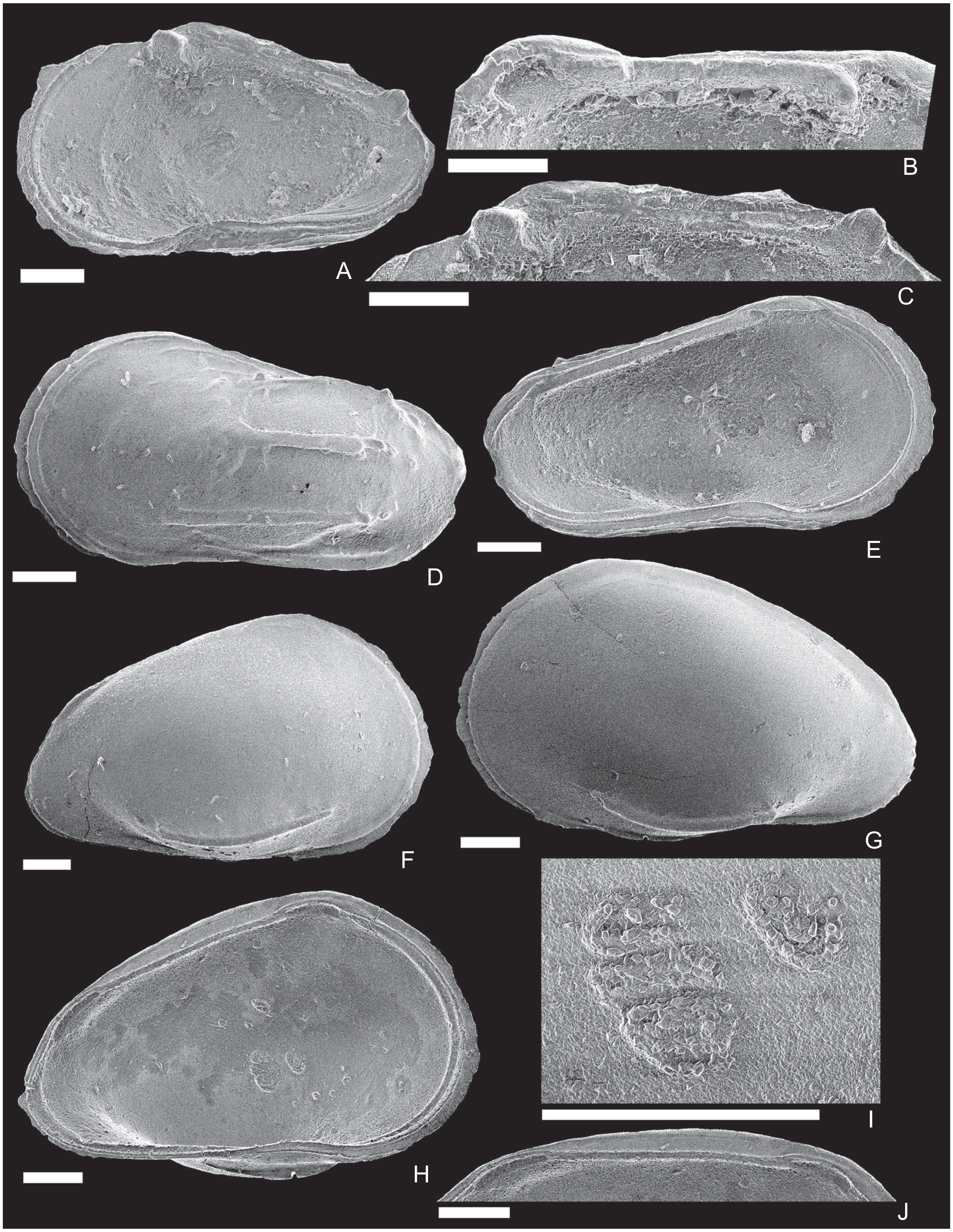

Figure 6. SEM images of ostracode species. **A–C,** *Phacorhabdotus flabellicarinus* sp. nov.; A, internal view of adult RV (SIO-BIC-C12187, paratype); B, hingement of adult LV (MPC-29116, holotype); C, hingement of adult RV (SIO-BIC-C12187, paratype); **D, E,** *Phacorhabdotus inaequicostata* Colin and Donze in Donze *et al.*, 1982 (MPC-29115); D, external view of adult LV; E, internal view of adult LV; **F–J,** *Pterygocythere* sp.; F, external view of juvenile RV (SIO-BIC-C12165); G, external view of juvenile LV (MPC-29106); H, internal view of juvenile LV (MPC-29106); I, muscle scars of juvenile LV (MPC-29106); J, hingement of juvenile LV (MPC-29106). All scale bars indicate 100 μm.

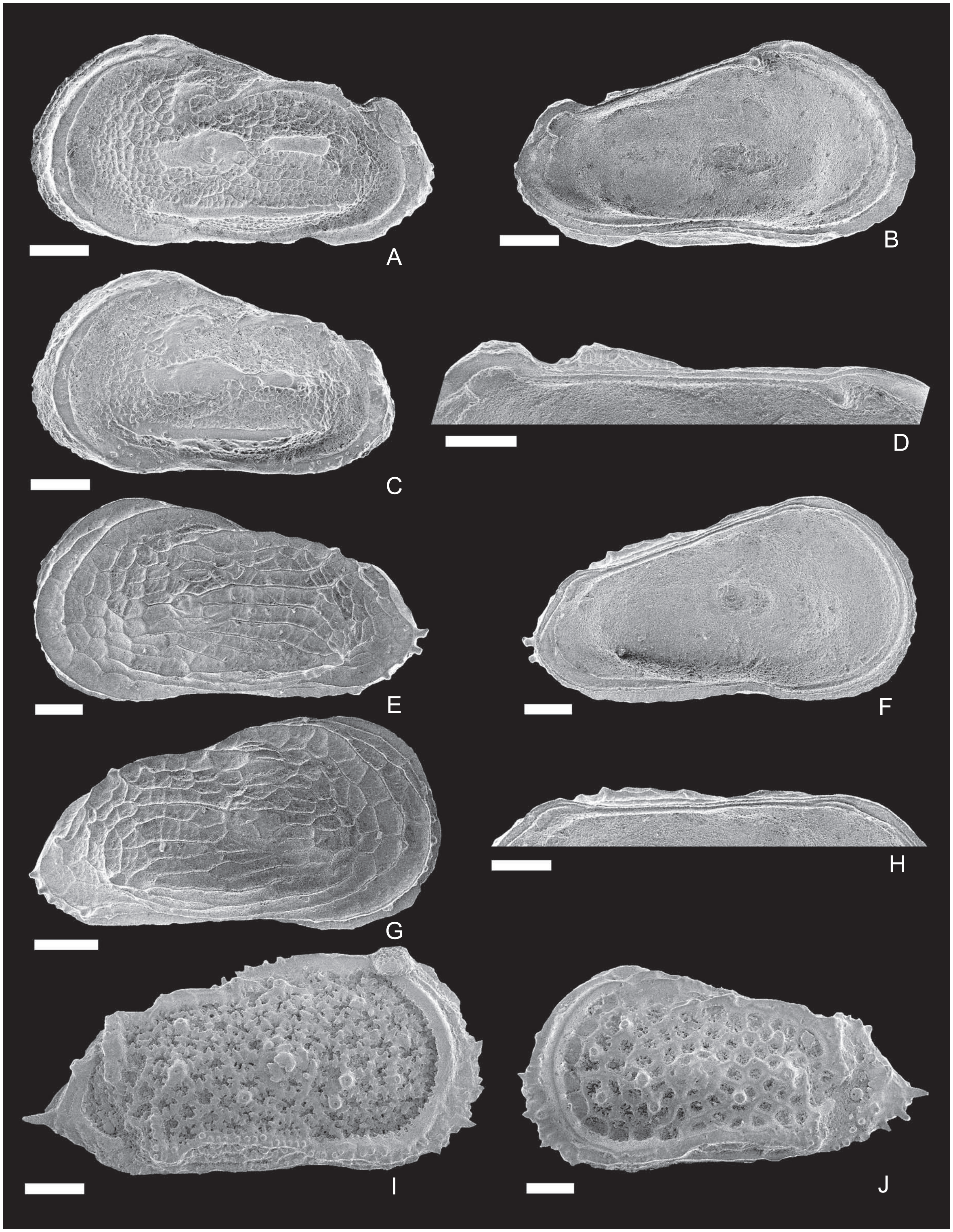

Figure 7. SEM images of ostracode species. **A–D,** *Ryugucivis blumi* sp. nov.; A, external view of adult LV (MPC-29121, holotype); B, internal view of adult LV (MPC-29121, holotype); C, external view of adult LV (SIO-BIC-C12161, paratype); D, hingement of adult LV (MPC-29121, holotype); **E–H,** *Rygucivis* sp.; E, external view of adult LV (MPC-29122); F, internal view of adult LV (MPC-29122); G, external view of adult RV (SIO-BIC-C12189); H, hingement of of adult LV (MPC-29122); **I, J,** *Trachyleberidea cronini* sp. nov.; I, external view of adult male RV (SIO-BIC-C12166, paratype); J, external view of adult female LV (MPC-29124, holotype). All scale bars indicate 100 μm.

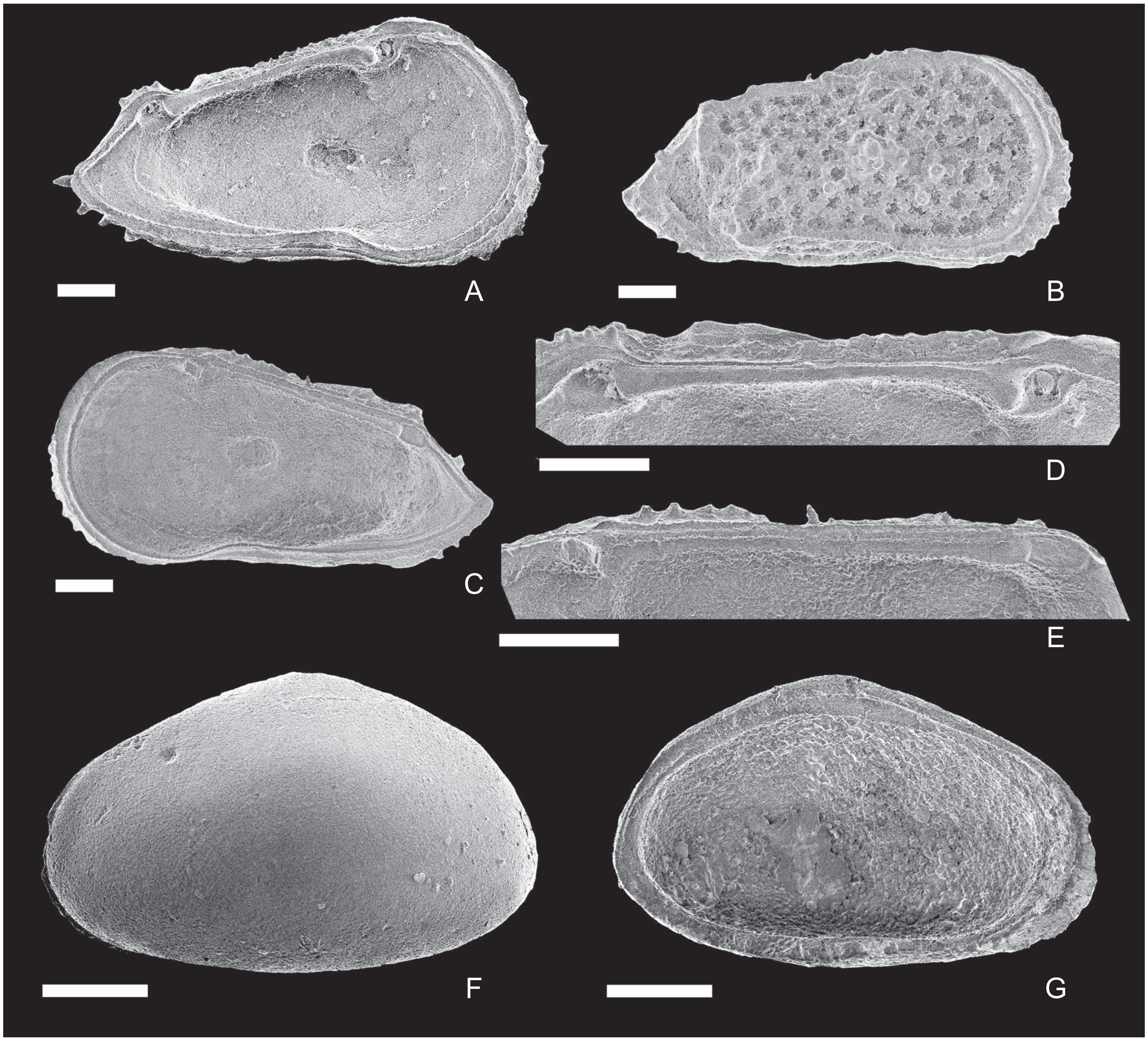

Figure 8. SEM images of ostracode species. **A–E**, *Trachyleberidea cronini* sp. nov.; A, internal view of adult female LV (MPC-29124, holotype); B, external view of adult male RV (MPC-29125, paratype); C, internal view of adult male RV (MPC-29125, paratype); D, hingement of adult female LV (MPC-29124, holotype); E, hingement of adult male RV (MPC-29125, paratype); **F, G**, *Platyleberis* sp. (MPC-29118); F, external view of adult LV; G, internal view of adult LV. All scale bars indicate 100 µm.

and Yamaguchi *et al*. (2012) and are deposited at Richard D. Norris's laboratory at SIO. Abbreviations: LV = left valve, RV = right valve, *L* = length, and *H* = height.

Systematic description of selected taxa

We identify 14 species of the families Eucytheridae, Krithidae, Thaerocytheridae, Trachyleberididae, and Xestoleberididae, including five new species.

Family Eucytheridae Puri, 1953
Genus ***Eucythere*** Brady, 1868
Eucythere sp.

Figures 3A, B, 9A, 11A

Description.—Carapace robust and small (479 µm long). In external view, lateral outline subtrapezoidal: anterior margin round; posterior margin sharply round; dorsal margin slightly arched and sloping posteriorly; ventral margin curved. Maximum length across posterodorsal

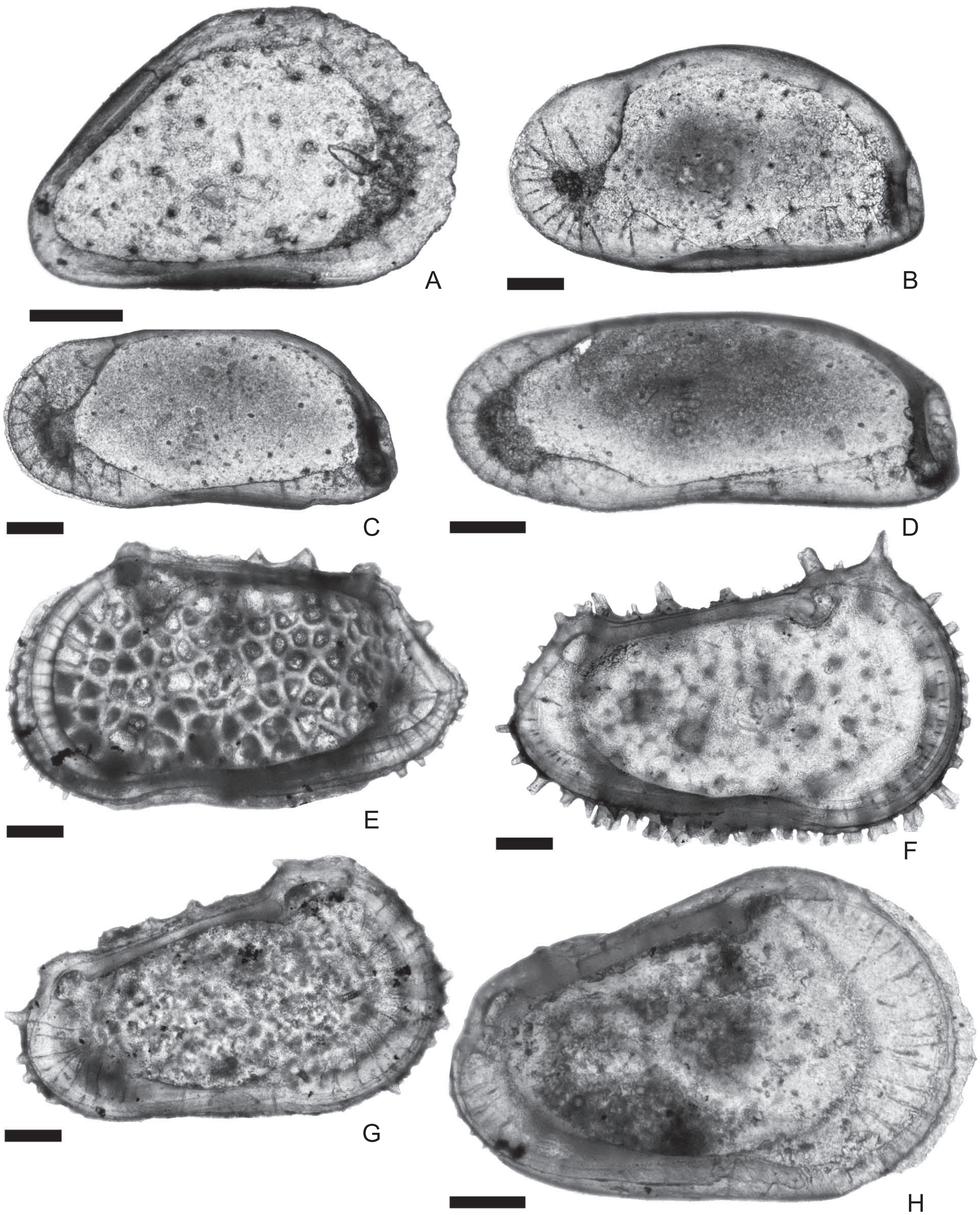

Figure 9. Light microscopic images of internal views of ostracode species in transmitted light. **A,** *Eucythere* sp. (MPC-29107); **B,** *Krithe crassicaudata* Bold, 1946 (MPC-29111); **C,** *Krithe dolichodeira* Bold, 1946 s.l. (MPC-29112); **D,** *Krithe* sp. (SIO-BIC-C12182); **E,** *Poseidonamicus norrisi* sp. nov. (MPC-29119); **F,** *Croninocythereis clavae* sp. nov. (MPC-29114); **G,** *Herrigocythere* sp. (MPC-29105); **H,** *Phacorhabdotus flabellicarinus* sp. nov. (MPC-29116). All scale bars indicate 100 μm.

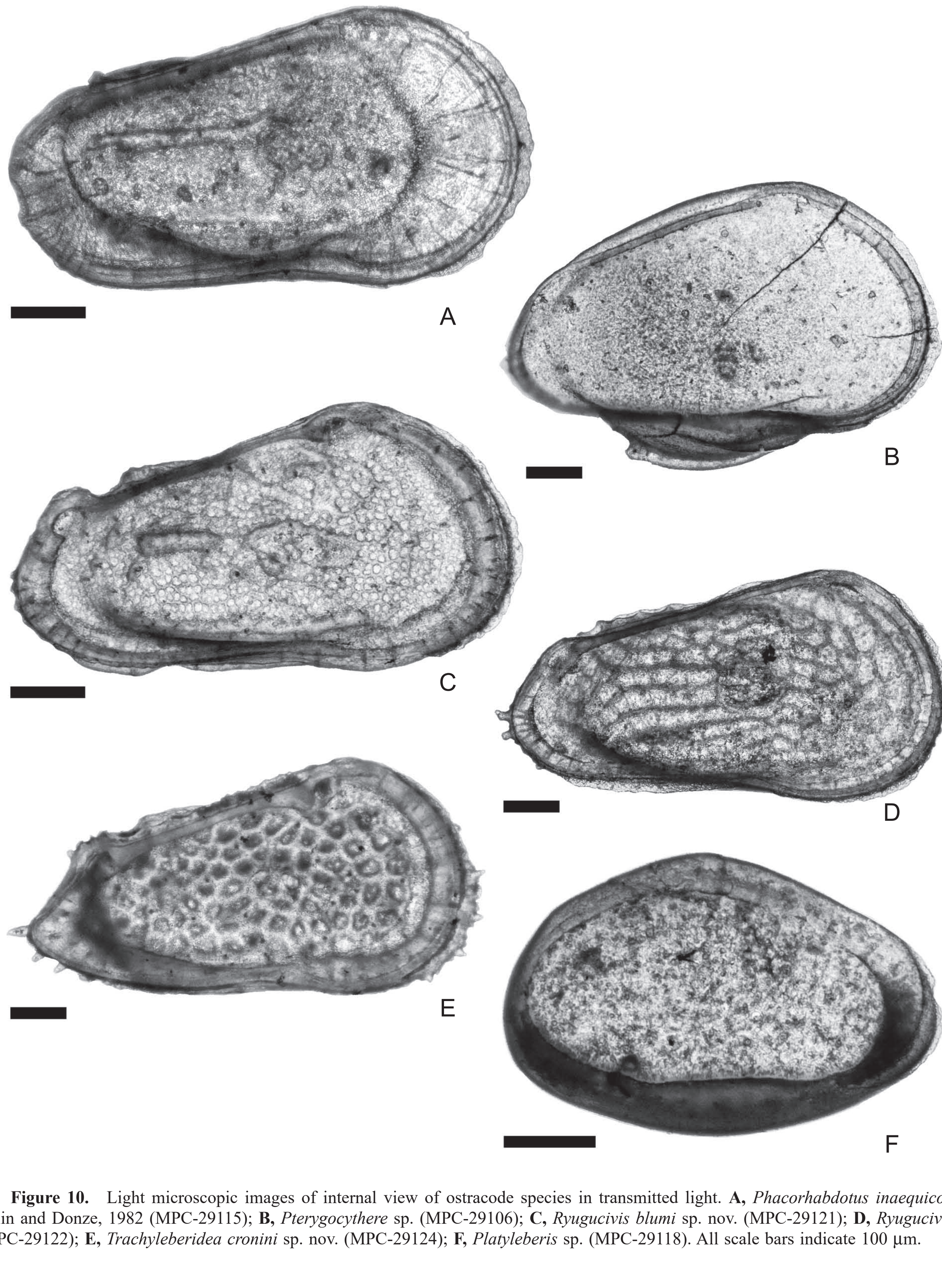

Figure 10. Light microscopic images of internal view of ostracode species in transmitted light. **A,** *Phacorhabdotus inaequicostata* Colin and Donze, 1982 (MPC-29115); **B,** *Pterygocythere* sp. (MPC-29106); **C,** *Ryugucivis blumi* sp. nov. (MPC-29121); **D,** *Ryugucivis* sp. (MPC-29122); **E,** *Trachyleberidea cronini* sp. nov. (MPC-29124); **F,** *Platyleberis* sp. (MPC-29118). All scale bars indicate 100 μm.

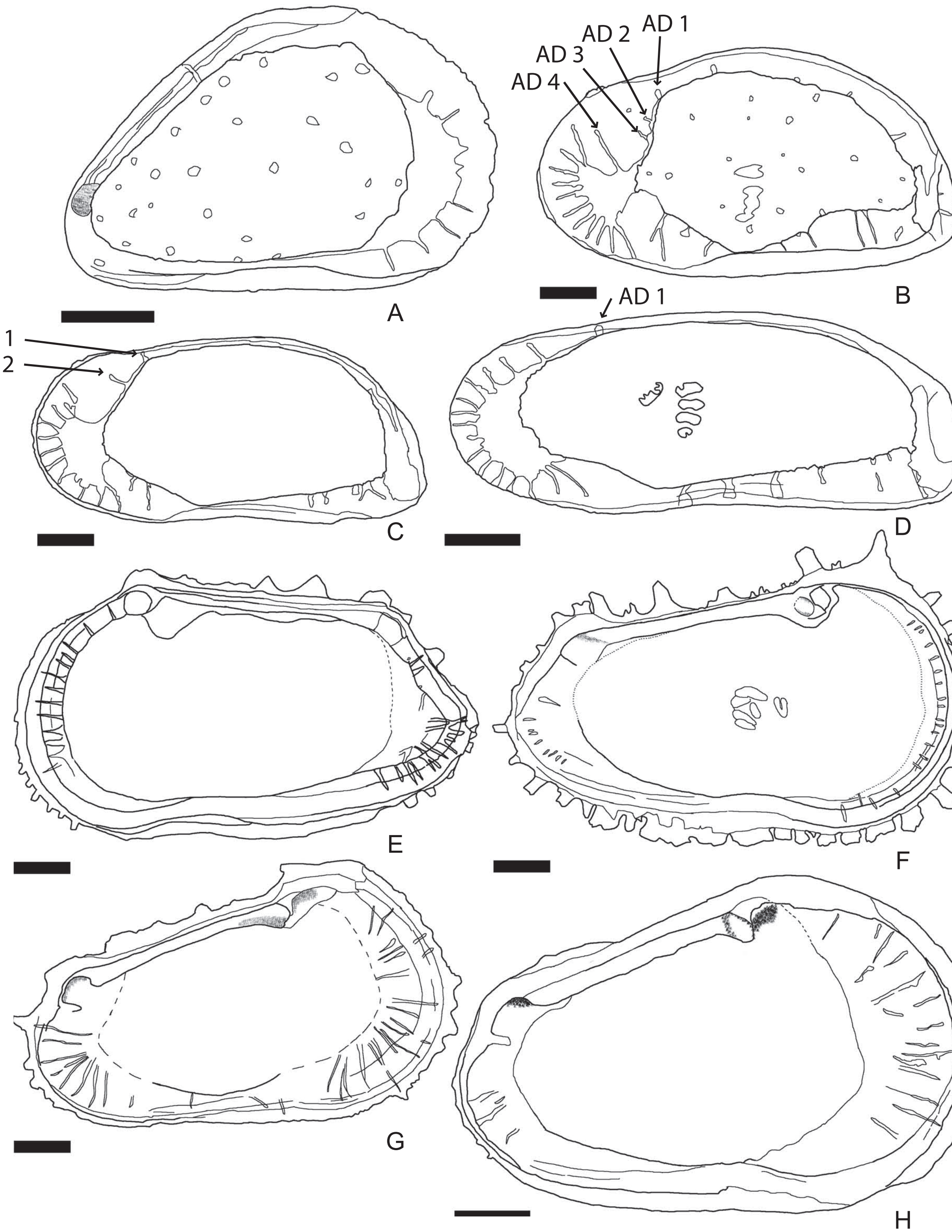

Figure 11. Sketches of the internal structures of ostracode species. **A,** *Eucythere* sp. (MPC-29107); **B,** *Krithe crassicaudata* Bold, 1946 (MPC-29111); **C,** *Krithe dolichodeira* Bold, 1946 s.l. (MPC-29112); **D,** *Krithe* sp. (SIO-BIC-C12182); **E,** *Poseidonamicus norrisi* sp. nov. (MPC-29119); **F,** *Croninocythereis clavae* sp. nov. (MPC-29114); **G,** *Herrigocythere* sp. (MPC-29105); **H,** *Phacorhabdotus flabellicarinus* sp. nov. (MPC-29116). All scale bars indicate 100 μm. The code for the anterodorsal radial pore canal (AD 1–4) was designed by Coles *et al.* (1994).

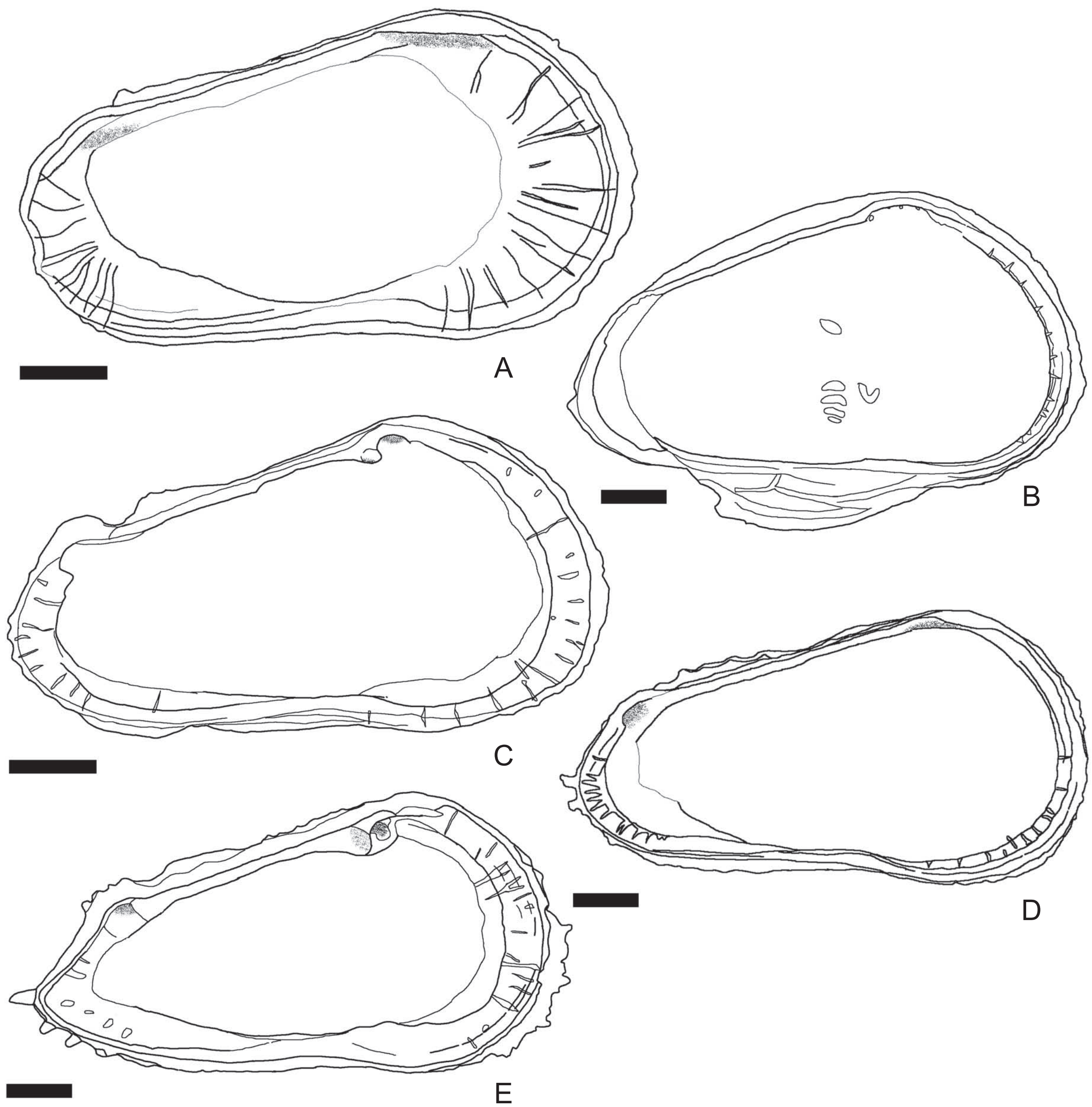

Figure 12. Sketches of the internal structures of ostracode species. **A,** *Phacorhabdotus inaequicostata* Colin and Donze, 1982 (MPC-29115); **B,** *Pterygocythere* sp. (MPC-29106); **C,** *Ryugucivis blumi* sp. nov. (MPC-29121); **D,** *Ryugucivis* sp. (MPC-29122); **E,** *Trachyleberidea cronini* sp. nov. (MPC-29124). All scale bars indicate 100 µm.

corner; maximum height across anterodorsal corner. Surface smooth with sieve pores. In internal view, lophodont-type hingement: in LV, anterior element is a socket that gradually connects to median bar; smooth median bar; posterior element is a half round socket. Anterior marginal zone width more than 10% of the maximum valve length. Vestibulum on anterior marginal zone. Eight anterior marginal pore canals short and straight, stretching from vestibulum.

Material.—MPC-29107, RV, adult, 342-U1407A-22X-1W, 20–22, Danian.

Measurement.—Table 1.

Remarks.—This species is similar to *Eucythere paralaevis* Coles and Whatley, 1989 and *E. triangula* Whatley and Coles, 1987 in lateral outline and size. It differs from *E. paralaevis* in having fewer anterior marginal pore canals and lacking horizontal carinae on the ventral area, and from *E. triangula* in having a smooth

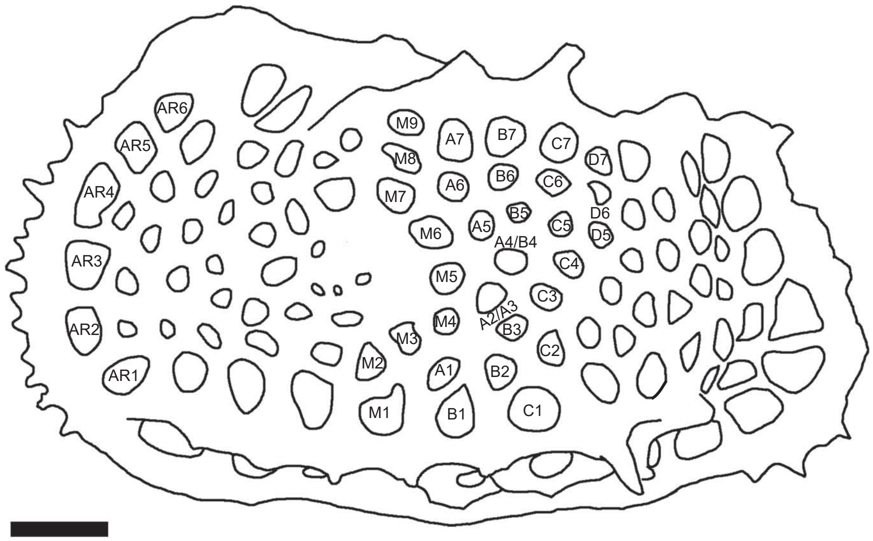

Figure 13. Drawing of the external view of *Poseidonamicus norrisi* sp. nov. (SIO-BIC-C12162). The scale bar indicates 100 μm. The code of fossae was designed by Hunt (2007).

surface in the central and posterior areas. *E. paralaevis* was originally described from upper Oligocene sediments at DSDP Site 549 and is found in Eocene–Oligocene sediments. *E. triangula* was originally described from upper Quaternary sediments at DSDP Sites 607 and 608, North Atlantic.

Family Krithidae Mandelstam cited in Bubikyan, 1958
Genus ***Krithe*** Brady, Crosskey, and Robertson, 1874
Krithe crassicaudata Bold, 1946

Figures 3C, D, 9B, 11B

For comprehensive pre-1994 synonymy see Coles *et al*. (1994)

Krithe crassicaudata Bold. Yamaguchi and Norris, 2012, p. 36, figs. 3.11, 4.1; Yamaguchi *et al*., 2012, fig. 3.

Material.—MPC-29111, RV, adult, 342-U1407C-16X-3W, 62–64, Thanetian; SIO-BIC-C12181, LV, adult, 342-U1407C-15X-7W, 20–22, Thanetian.

Measurement.—Table 1.

Remarks.—We recognize the characters of *Krithe crassicaudata* as follows: subovate lateral outline, four anterodorsal radial pore canals with long AD 4, “mushroom”-shaped anterior vestibulum, and eleven anterior radial pore canals.

Krithe dolichodeira Bold, 1946 *sensu lato*

Figures 3E, F, 9C, 11C

For comprehensive pre-1999 synonymy see Coles *et al*. (1994) and Ayress *et al*. (1999)

Krithe dolichodeira Bold. Bergue, 2006, fig. 1C, D; Bergue *et al*. 2006, fig. 6P; Bergue and Coimba, 2008, fig. 1G; Yasuhara *et al*. 2014, p. 352, figs. 4.5, 4.6; Alvarez Zarikian, 2015, pl. 2, figs. 1–3; DeNinno *et al*., 2015, pl. 1, fig. 8; Martinez-Garcia *et al*., 2015, pl. 11, fig. 17.

Material.— SIO-BIC-C12183, RV, adult, 342-U1407C-15X-6W, 70–72, Thanetian; MPC-29112, RV, adult, 342-U1407C-15X-7W, 20–22, Thanetian.

Measurement.—Table 1.

Remarks.—We found characters of *Krithe dolichodeira* as follows: subquadrate lateral outline, two anterodorsal radial pore canals with short AD 1 and long AD 2, “mushroom”-shaped anterior vestibulum, and eleven anterior radial pore canals. The stratigraphic range of the taxon extends to the upper Paleocene.

Krithe sp.

Figures 3G, H, 9D, 11D

Material.—MPC-29113, RV, adult, 342-U1407C-14X-1W, 106–108, Thanetian; SIO-BIC-C12182, RV, adult, 342-U1407C-15X-7W, 20–22, Thanetian.

Measurement.—Table 1.

Remarks.—The following characters are shared with *K. regulare* Coles, Whatley, and Moguliesvky, 1994: subrectangular lateral outline and a short AD 1. However, its vestibulum is not “mushroom”-shaped, but “pocket”-shaped. Hence, we consider the taxon as a species that is

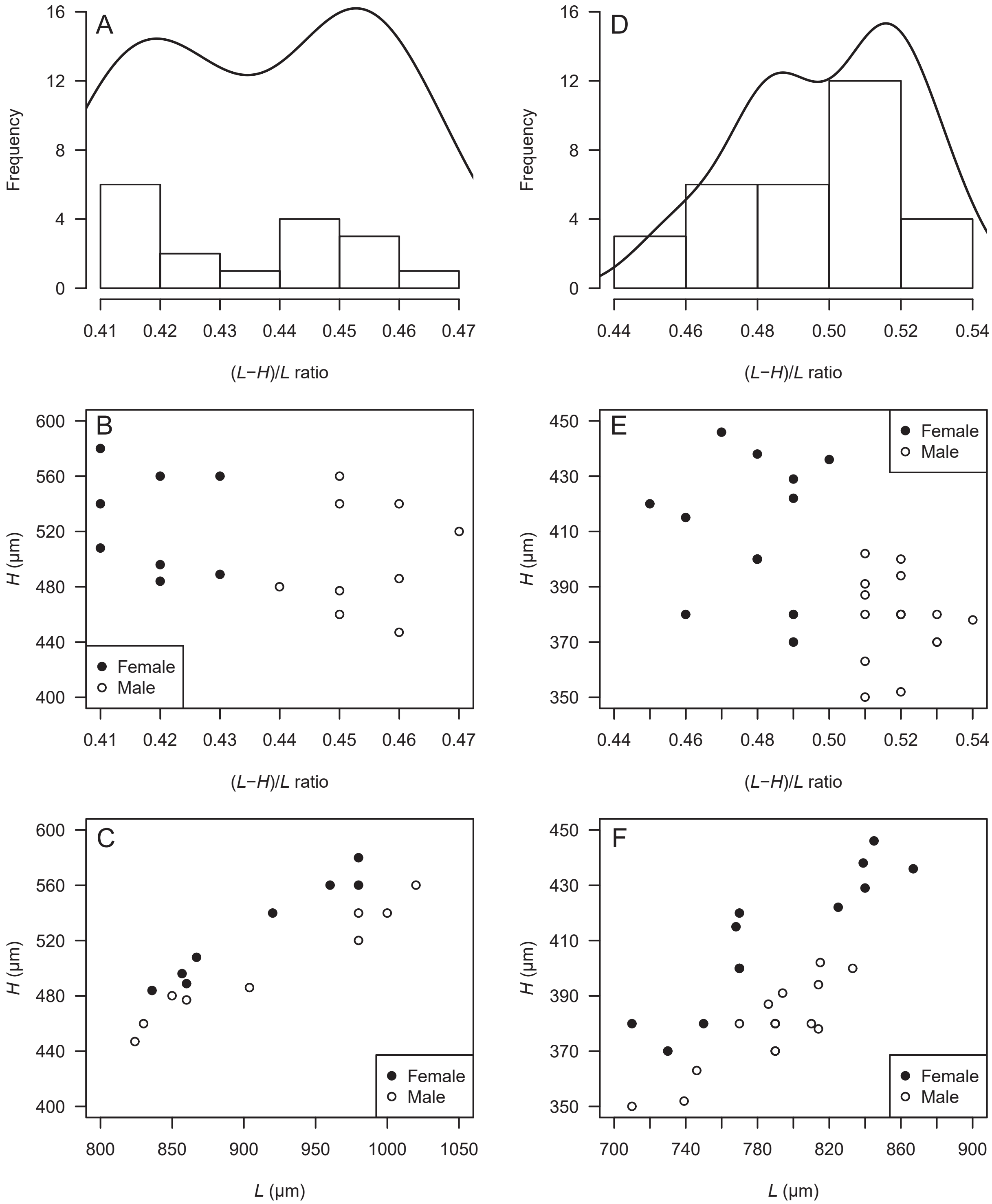

Figure 14. Measurements of *Poseidonamicus norrisi* sp. nov. and *Trachyleberidea cronini* sp. nov. **A–C,** *P. norrisi* sp. nov.: A, histogram and Gaussian kernel density estimation of the (*L*−*H*)/*L* ratio; B, plot of the (*L*−*H*)/*L* ratio and L; C, plot of L and H. **D–F,** *T. cronini* sp. nov.; D, histogram and Gaussian kernel density estimation of the (*L*−*H*)/*L* ratio; E, plot of the (*L*−*H*)/*L* ratio and L; F, plot of *L* and *H*. Details of the measurements are shown in Table 1.

Table 1. Measurements and features of the specimens, and sediment samples with the specimens. The numerical ages were calculated using the calcareous nannofossil biostratigraphy (Norris *et al*., 2014; Yamaguchi *et al*., submitted). Abbreviations: H = holotype, P = paratype, R = right valve, L = left valve, A = adult, J = juvenile, F = female, M = male. *Poseidonamicus norrisi* sp. nov. and *Trachyleberidea cronini* sp. nov. from DSDP Site 401 were measured at ×50 magnification, using a micrometer (Yamaguchi *et al*., 2012).

Catalog number	Species	Type	Valve types	Growth stage/sex	Length (µm)	Height (µm)	Sample identifier	Depth of sample (mbsf)	(mcd)	Age	(Ma)	Figure	Remarks
SIO-BIC-C12168	*Croninocythereis clavae* sp. nov.	P	R	A	754	456	342-U1407C-14X-1W, 70–72	122.70	146.47	Thanelian	57.439	4I	
MPC-29114	*Croninocythereis clavae* sp. nov.	H	L	A	848	565	342-U1407C-15X-5W, 72–74	138.32	162.30	Thanelian	59.091	4H, 5A–C, 9F, 11F	
SIO-BIC-C12180	*Croninocythereis clavae* sp. nov.	P	R	A	873	509	342-U1407C-15X-6W, 116–118	140.26	164.24	Thanelian	59.223		
MPC-29107	*Eucythere* sp.		R	A	479	309	342-U1407A-22X-1W, 20–22	174.50	204.65	Danian	62.695	3A, B, 9A, 11A	
SIO-BIC-C12169	*Herrigocythere* sp.		R	A	707	371	342-U1407C-17X-6W, 33–35.5	158.63	184.57	Selandian	60.485		
SIO-BIC-C12170	*Herrigocythere* sp.		R	A	698	352	342-U1407A-21X-3W, 20–22	167.90	198.32	Selandian	61.313		
MPC-29105	*Herrigocythere* sp.		L	A	816	486	342-U1407C-20X-6W, 45–47.5	182.95	216.33	Maastrichtian	66.108	5D, E, 9G, 11G	
MPC-29111	*Krithe crassicaudata* Bold, 1946		R	A	755	411	342-U1407C-16X-3W, 62–64	144.82	169.60	Thanelian	59.585	9B, 11B	
SIO-BIC-C12181	*Krithe crassicaudata* Bold, 1946		L	A	826	460	342-U1407C-15X-7W, 20–22	140.80	164.78	Thanelian	59.260	3C, D	
SIO-BIC-C12183	*Krithe dolichodeira* Bold, 1946 s.l.		R	A	706	304	342-U1407C-15X-6W, 70–72	139.80	163.78	Thanelian	59.192		
MPC-29112	*Krithe dolichodeira* Bold, 1946 s.l.		R	A	715	347	342-U1407C-15X-7W, 20–22	140.80	164.78	Thanelian	59.260	3E, F, 9C, 11C	
MPC-29113	*Krithe* sp.		R	A	730	351	342-U1407C-14X-1W, 106–108	123.06	146.83	Thanelian	57.478	3G, H	
SIO-BIC-C12182	*Krithe* sp.		R	A	682	281	342-U1407C-15X-7W, 20–22	140.80	164.78	Thanelian	59.260	9D, 11D	
MPC-29116	*Phacorhabdotus flabellicarinus* sp. nov.	H	L	A	722	452	342-U1407A-22X-2W, 20–22	176.00	206.15	Danian	63.268	5F, G, 6B, 9H, 11H	
SIO-BIC-C12187	*Phacorhabdotus flabellicarinus* sp. nov.	P	R	A	665	377	342-U1407A-22X-4W, 124–126	180.04	210.19	Danian	64.278	5H, 6A, C	
MPC-29117	*Phacorhabdotus flabellicarinus* sp. nov.	P	L	A	648	392	342-U1407C-17X-5W, 35–37.5	157.15	183.09	Selandian	60.396		
SIO-BIC-C12188	*Phacorhabdotus flabellicarinus* sp. nov.	P	L	A	698	444	342-U1407A-22X-4W, 124–126	180.04	210.19	Danian	64.278		
MPC-29115	*Phacorhabdotus inaequicostata* Colin and Donze, 1982		L	A	796	390	342-U1407B-19X-3W, 82–84	188.42	216.32	Maastrichtian	66.107	6D, E, 10A, 12A	
MPC-29118	*Platyleberis* sp.		L	A	484	299	342-U1407C-17X-4W, 68–70	155.98	181.92	Selandian	60.326	8F, G, 10F	
SIO-BIC-C12172	*Platyleberis* sp.		R	A	502	295	342-U1407C-18X-3W, 15–17	163.55	189.58	Selandian	60.787		
SIO-BIC-C12162	*Poseidonamicus norrisi* sp. nov.	P	L	A/F	867	508	342-U1407C-17X-3W, 70–72	154.50	180.44	Selandian	60.237	4A, 13	
SIO-BIC-C12163	*Poseidonamicus norrisi* sp. nov.	P	L	A/F	857	496	342-U1407C-18X-4W, 72–74	165.62	191.65	Selandian	60.911		
MPC-29119	*Poseidonamicus norrisi* sp. nov.	H	R	A/M	860	477	342-U1407C-18X-4W, 72–74	165.62	191.65	Selandian	60.911	4B, C, G, 9E, 11E	
MPC-29120	*Poseidonamicus norrisi* sp. nov.	P	L	A/F	836	484	342-U1407C-18X-4W, 105–107.5	165.95	191.98	Selandian	60.931	4D–F	
–	*Poseidonamicus norrisi* sp. nov.		L	A/M	904	486	342-U1407C-18X-6W, 70–72	168.60	194.63	Selandian	61.091		
–	*Poseidonamicus norrisi* sp. nov.		L	A/F	860	489	342-U1407C-18X-7W, 20–22	169.41	195.44	Selandian	61.139		
–	*Poseidonamicus norrisi* sp. nov.		L	A/F	824	447	342-U1407C-20X-4W, 4–6	179.54	212.92	Danian	64.960		
–	*Poseidonamicus norrisi* sp. nov.		L	A/M	1020	560	48-401-14R-4, 34–35	203.34	–	Thanetian			
–	*Poseidonamicus norrisi* sp. nov.		R	A/M	980	540	48-401-14R-4, 35–36	203.35	–	Thanetian			
–	*Poseidonamicus norrisi* sp. nov.		L	A/M	850	480	48-401-14R-4, 50–51	203.50	–	Thanetian			
–	*Poseidonamicus norrisi* sp. nov.		L	A/M	980	580	48-401-14R-4, 50–51	203.50	–	Thanetian			
–	*Poseidonamicus norrisi* sp. nov.		R	A/M	960	560	48-401-14R-4, 65–66	203.65	–	Thanetian			
–	*Poseidonamicus norrisi* sp. nov.		R	A/M	830	460	48-401-14R-4, 70–71	203.70	–	Thanetian			
–	*Poseidonamicus norrisi* sp. nov.		R	A/M	980	520	48-401-14R-4, 70–71	203.70	–	Thanetian			
–	*Poseidonamicus norrisi* sp. nov.		R	A/M	1000	540	48-401-14R-3, 133–134	204.33	–	Thanetian			
–	*Poseidonamicus norrisi* sp. nov.		L	A/F	980	560	48-401-14R-4, 140–141	204.40	–	Thanetian			
–	*Poseidonamicus norrisi* sp. nov.		L	A/M	920	540	48-401-14R-3, 143–145	204.43	–	Thanetian			Fig. 3.20 of Yamaguchi and Norris (2012)
MPC-29106	*Pterygocythere* sp.		L	J	812	476	342-U1407C-14X-6W, 21–23	129.71	153.48	Thanetian	58.202	6G–J, 10B, 12B	
SIO-BIC-C12164	*Pterygocythere* sp.		R	J	804	460	342-U1407C-14X-6W, 21–23	129.71	153.48	Thanetian	58.202		
SIO-BIC-C12165	*Pterygocythere* sp.		R	J	873	528	342-U1407B-19X-3W, 22–24	187.82	215.72	Maastrichtian	66.044	6F	
SIO-BIC-C12160	*Ryugucivis blumi* sp. nov.	P	L	A	629	340	342-U1407C-20X-4W, 44–46	179.94	213.32	Danian	65.060		
SIO-BIC-C12161	*Ryugucivis blumi* sp. nov.	P	L	A	636	354	342-U1407C-20X-4W, 49–51	179.99	213.37	Danian	65.073	7C	
MPC-29121	*Ryugucivis blumi* sp. nov.	H	L	A	702	367	342-U1407C-18X-3W, 122–124	164.62	190.65	Selandian	60.851	7A, B, D, 10C, 12C	
MPC-29122	*Ryugucivis* sp.		L	J	834	428	342-U1407B-19X-3W, 102–104	188.62	216.52	Maastrichtian	66.127	7E, F, H, 10D, 12D	
SIO-BIC-C12189	*Ryugucivis* sp.		R	J	662	344	342-U1407B-19X-3W, 122–124	188.82	216.72	Maastrichtian	66.148	7G	
MPC-29123	*Ryugucivis* sp.		L	J	625	342	342-U1407B-19X-3W, 42–44	188.02	215.92	Maastrichtian	66.065		
SIO-BIC-C12190	*Ryugucivis* sp.		L	J	690	358	342-U1407B-19X-3W, 82–84	188.42	216.32	Maastrichtian	66.107		
MPC-29124	*Trachyleberidea cronini* sp. nov.	H	L	A/F	867	436	342-U1407C-20X-5W, 34–36	181.34	214.72	Danian	65.410	7J, 8A, D, 10E, 12E	
SIO-BIC-C12166	*Trachyleberidea cronini* sp. nov.	P	R	A/M	794	391	342-U1407C-17X-2W, 114–116	153.44	179.38	Selandian	60.173	7I	
SIO-BIC-C12167	*Trachyleberidea cronini* sp. nov.	P	L	A/F	839	438	342-U1407A-21X-3W, 20–22	168.40	198.32	Selandian	61.313		
MPC-29125	*Trachyleberidea cronini* sp. nov.	P	R	A/M	786	387	342-U1407C-17X-4W, 68–70	155.98	181.92	Selandian	60.326	8B, C, E	
–	*Trachyleberidea cronini* sp. nov.		R	A/F	794	391	342-U1407C-17X-2W, 114–116	153.44	179.38	Selandian	60.173		
–	*Trachyleberidea cronini* sp. nov.		R	A/F	786	387	342-U1407C-17X-4W, 68–70	155.98	181.92	Selandian	60.326		
–	*Trachyleberidea cronini* sp. nov.		L	A/M	839	438	342-U1407A-21X-3W, 20–22	167.90	198.32	Selandian	61.313		
–	*Trachyleberidea cronini* sp. nov.		L	A/M	867	436	342-U1407C-20X-5W, 34–36	181.34	214.72	Danian	65.410		
–	*Trachyleberidea cronini* sp. nov.		R	A/F	750	380	48-401-14R-1, 81–83	199.31	–	Ypresian	–		Yamaguchi *et al.* (2012)
–	*Trachyleberidea cronini* sp. nov.		L	A/F	770	380	48-401-14R-2, 8–10	200.08	–	Ypresian	–		Yamaguchi *et al.* (2012)
–	*Trachyleberidea cronini* sp. nov.		L	A/F	770	400	48-401-14R-2, 8–10	200.08	–	Ypresian	–		Yamaguchi *et al.* (2012)
–	*Trachyleberidea cronini* sp. nov.		R	A/F	770	400	48-401-14R-2, 8–10	200.08	–	Ypresian	–		Yamaguchi *et al.* (2012)
–	*Trachyleberidea cronini* sp. nov.		L	A/F	770	400	48-401-14R-2, 8–10	200.08	–	Ypresian	–		Yamaguchi *et al.* (2012)
–	*Trachyleberidea cronini* sp. nov.		R	A/F	770	400	48-401-14R-2, 8–10	200.08	–	Ypresian	–		Yamaguchi *et al.* (2012)
–	*Trachyleberidea cronini* sp. nov.		R	A/F	790	380	48-401-14R-2, 31–33	200.31	–	Ypresian	–		Yamaguchi *et al.* (2012)
–	*Trachyleberidea cronini* sp. nov.		L	A/F	790	370	48-401-14R-3, 21–23	201.71	–	Ypresian	–		Yamaguchi *et al.* (2012)
–	*Trachyleberidea cronini* sp. nov.		R	A/F	790	370	48-401-14R-3, 21–23	201.71	–	Ypresian	–		Yamaguchi *et al.* (2012)
–	*Trachyleberidea cronini* sp. nov.		R	A/F	790	380	48-401-14R-3, 108–110	202.58	–	Thanetian	–		Yamaguchi *et al.* (2012)
–	*Trachyleberidea cronini* sp. nov.		R	A/F	710	350	48-401-14R-3, 112–114	202.62	–	Thanetian	–		Yamaguchi *et al.* (2012)
–	*Trachyleberidea cronini* sp. nov.		L	A/F	730	370	48-401-14R-3, 143–145	202.93	–	Thanetian	–		Yamaguchi *et al.* (2012)
–	*Trachyleberidea cronini* sp. nov.		R	A/F	730	370	48-401-14R-3, 143–145	202.93	–	Thanetian	–		Yamaguchi *et al.* (2012)
–	*Trachyleberidea cronini* sp. nov.		R	A/F	790	380	48-401-14R-4, 24–25	203.24	–	Thanetian	–		Yamaguchi *et al.* (2012)
–	*Trachyleberidea cronini* sp. nov.		L	A/F	770	420	48-401-14R-4, 32–33	203.32	–	Thanetian	–		Yamaguchi *et al.* (2012)
–	*Trachyleberidea cronini* sp. nov.		L	A/F	710	380	48-401-14R-4, 45–46	203.45	–	Thanetian	–		Yamaguchi *et al.* (2012)
–	*Trachyleberidea cronini* sp. nov.		L	A/F	810	380	48-401-14R-4, 70–71	203.70	–	Thanetian	–		Yamaguchi *et al.* (2012)

comparable with *K. regulare*.

Family Thaerocytheridae Hazel, 1967
Genus ***Poseidonamicus*** Benson, 1972 emend. Whatley, Downing, Kesler, and Harlow, 1986
Poseidonamicus norrisi sp. nov.

Figures 4A–G, 9E, 11E, 13

Poseidonamicus sp. Yamaguchi and Norris, 2012. p. 37, fig. 3.20.

Diagnosis.—A *Poseidonamicus* species characterized by the subrectangular lateral outline, finer reticulation on the central area, blunt four spines on the continuous dorsal ridge above the mural loop, and the A6 fossa dorsal to both the M6 and A5 fossae.

Description.—Carapace robust and large (824–1020 µm long). In external view, lateral outline subrectangular: anterior margin round; posterior margin obtuse, tapering near ventral one-third forming a caudal process; dorsal margin slightly curved and sloping posteriorly; ventral margin curved. Maximum length across anterodorsal corner; maximum height across middle of valve. Posterior area flattened. Central area before posterodorsal corner swollen. Ventral ridge developed. Marginal rims developed along anterior and posterior margins. Marginal denticles along anterior margin and ventral half of posterior margin. Dorsal ridge developed above mural loop. Surface ornamented with spines and reticulation. Sharp conjunctive spines on ventral ridge. Long spines near posterior terminal of ventral ridge. Four short blunt spines arranged on dorsal ridge. Reticulation composed of round, rectangular, and polygonal fossae framed by blunt muri. Six anterior fossae arranged along anterior marginal rim in LV and RV. Smaller round fossae on anterior and central areas. Larger rectangular fossae on posterior area. Eye tubercle prominent and connected with murus. Sexual dimorphism distinctive. Male form more elongated than female form: $(L-H)/L$ ratio ≤ 0.43 in female form; $(L-H)/L$ ratio > 0.43 in male form. In internal view, amphidont-type hingement: in LV, half round socket of anterior element; round tooth at anterior terminal of median bar; smooth median bar; half round socket of posterior element; in RV, round tooth of anterior element; half round hollow at anterior terminal of median groove, gradually connected to median groove; half round tooth of posterior element. Anterior marginal zone width less than 10% of the maximum valve length. Anterior marginal pore canals moderately long and straight; posterior marginal pore canals moderately long and straight, often furcated. Thirteen pore canals on anterior marginal zone; eleven pore canals on posterior marginal zone. Striae on anterior marginal zone.

Etymology.—In honor of Richard D. Norris (Scripps Institution of Oceanography, University of California, San Diego), who studies paleoceanography and planktic foraminifers and led IODP Exp 342 as one of the Co-Chief Scientists.

Measurement.—Figure 14, Table 1.

Types.—Holotype: MPC-29119, RV, adult, male, 342-U1407C-18X-4W, 72–74, Selandian. Paratypes: SIO-BIC-C12162, LV, adult, female, 342-U1407C-17X-3W, 70–72, Selandian; SIO-BIC-C12163, LV, adult, female, 342-U1407C-18X-4W, 72–74, Selandian; MPC-29120, LV, adult, female, 342-U1407C-18X-4W, 105–107.5, Selandian.

Other examined materials.—Three adult specimens from Site U1407 and ten adult specimens from DSDP Site 401.

Occurrence.—Upper Paleocene sediments at DSDP Site 401, North Atlantic (Yamaguchi and Norris, 2012); middle Paleocene sediments at IODP Site U1407 (this study).

Remarks.—Other characters formulated by Hunt (2007) and their status with regard to this new species are shown in Figure 13 and Appendix A.

Poseidonamicus norrisi sp. nov. is similar to *P. panopsus* Whatley and Dingle, 1989 in lateral outline and the pattern of reticulation, but is distinguished by having finer reticulation in the central area, four blunt spines on the continuous dorsal ridge above the mural loop, and the A6 fossa dorsal to both the M6 and A5 fossae (Figure 13; Appendix A). *Poseidonamicus panopsus* was originally described from Quaternary sediments. The new species is different from *P. major* Benson, 1972, the type of the genus, in having rounder fossae and a blunter dorsal ridge.

The new taxon disappears near the Paleocene/Eocene boundary at DSDP Site 401 (Yamaguchi and Norris, 2012).

Family Trachyleberididae Sylvester-Bradley, 1948
Genus ***Croninocythereis*** Yasuhara, Hunt, Okahashi, and Brandão, 2015
Croninocythereis clavae sp. nov.

Figures 4H, I, 5A–C, 9F, 11F

Diagnosis.—A *Croninocythereis* species characterized by scattered blunter tubercles such as clavae and bullae, four clavae arranged along the dorsal margin, three multifurcated tubercles in the central area, and five to six multifurcated tubercles in the ventral area.

Description.—Carapace robust and large (754–873 µm long). In external view, lateral outline subtrapezoidal: anterior round; posterior margin tapering; dorsal margin tapering with apex at anterodorsal corner; ventral margin curved with indent at anterior one-forth. Maximum length across the caudal process; maximum height across anterodorsal corner. Anterior marginal and posterior marginal rims blunt. Before posterior marginal rim, posterior area flattened and slightly depressed. Before posterodorsal corner, surface built up. Behind anterior marginal rim anterior area dressed and flattened. Subcentral tubercle prominent. Marginal denticles developed along anterior, ventral, and posterior margins. Clavae arranged as marginal denticles from ventral half of anterior margin to ventral half of posterior margin. Four clavae between anterodorsal and posterodorsal corners. Surface ornamentation consists of clavae, bullae, and short spines. Nine bullae arranged on anterior marginal rim. Three inflated multifurcated tubercles in middle of valve; one tubercle forming subcentral tubercle; two located behind subcentral tubercle. Short spines in central area. Five or six inflated multifurcated tubercles arranged along ventral margin. Short spines arranged vertically across posterodorsal corner. In internal view, amphidont-type hingement: in LV, this consists of a crenulated, round socket as anterior element; a smooth median bar with a round tooth at anterior end; and a rectangular socket as posterior element. Anterior marginal zone width less than 10% of maximum valve length. Marginal pore canals short and straight. Nineteen anterior and nine posterior marginal pore canals. Striae on anterior marginal zone. V-shaped frontal muscle scars. Adductor muscle scars formed by four rows of five ovate scars. In second top row, two scars arranged in inverted V-shape.

Etymology.—Named after the numerous clavae which ornament the valves, *clavae* being the feminine singular genitive of *clava*.

Types.—Holotype: MPC-29114, LV, adult, 342-U1407C-15X-5W, 72–74, Thanetian. Paratypes: SIO-BIC-C12168, RV, adult, 342-U1407C-14X-1W, 70–72, Thanetian; SIO-BIC-C12180, RV, adult, 342-U1407C-15X-6W, 116–118, Thanetian.

Measurements.—Table 1.

Remarks.—*Croninocythereis clavae* sp. nov. is different from *Legitimocythere acanthoderma* (Brady, 1880) and *L. geniculata* Mazzini, 2005 by having scattered spines, clavae, and bullae on the surface and a more tapered posterior margin. The latter species were originally described from Holocene sediments. The new species is distinguished from "*Acanthocythereis*" *dunelmensis* of Cronin and Compton-Gooding (1987) from a Pleistocene sample at DSDP Site 613, North Atlantic, by having distinct clavae along the ventral margin, two multifurcated tubercles as large as the subcentral tubercle in the central area, and blunter bullae on the anterior marginal rim and by lacking an eye tubercle.

Genus ***Herrigocythere*** Gründel, 1973
Herrigocythere sp.

Figures 5D, E, 9G, 11G

Herrigocythere sp. 2. Yasuhara *et al*., 2015, p. 139, fig. 11Q–R.

Description.—Carapace robust and large (698–816 μm long). In external view, lateral outline subrectangular: anterior and posterior margins round; dorsal margin slightly arched and sloping posteriorly; ventral margin slightly curved. Maximum length across apex of anterior margin; maximum height across anterodorsal corner. Blunt marginal rim developed along anterior margin. Seven clavae on anterior marginal rim. Marginal denticles developed along anterior and posterior margins. Subcentral tubercle indistinct. Three dorsal bullae arranged as follows: blunt node at dorsal bulla A; tubercles at dorsal bullae B and C. Gamos ridge developed in posterodorsal area. Surface ornamentation consists of reticulation formed by rectangular and polygonal fossae and fine muri. Secondary reticulation in anterior area. In internal view, amphidont-type hingement: in LV, this consists of a half round crenulated socket as anterior element; a smooth median bar with a round tooth at its anterior end; and a crenulated half round socket as posterior element. Anterior marginal zone width less than 10% of maximum valve length, having straight long marginal pore canals. Twenty-two pore canals on anterior margin; ten on posterior margin. Two or three rows of striae on anterior and ventral marginal zones.

Material.—MPC-29105, LV, adult, 342-U1407C-20X-6W, 45–47.5, Maastrichtian; SIO-BIC-C12169, RV, adult, 342-U1407C-17X-6W, 33–35.5, Selandian; SIO-BIC-C12170, RV, adult, 342-U1407A-21X-3W, 20–22, Selandian.

Occurrence.—Maastrichtian sediments at DSDP 111A, North Atlantic (Yasuhara *et al*., 2015); upper Cretaceous to middle Paleocene sediments at IODP U1407, North Atlantic (this study).

Measurement.—Table 1.

Remarks.—The taxon is possibly new. Because adult specimens occur rarely from the sediments and their preservation is not good, we do not propose a new scientific name. This taxon is similar to *Abyssocythere trinidadensis* (Bold, 1957) in the lateral outline, reticulation, and a developed anterior marginal rim, but is distinguished by having a blunter node at the dorsal bulla A, an undeveloped subcentral tubercular, and an undeveloped ventral lateral carina.

Genus ***Phacorhabdotus*** Howe and Laurencich, 1958
Phacorhabdotus flabellicarinus sp. nov.

Figures 5F–H, 6A–C, 9H, 11H

Phacorhabdotus sp. 3. Majoran, 1999, pl. 2, fig. 17; Guernet and Bellier, 2000, pl. 4, fig. 11.

Phacorhabdotus sp. Yamaguchi and Norris, 2012, fig. 3.17.

*Diagnosis.—*A *Phacorhabdotus* species characterized by having smooth surface, a blunt, fan-like horizontal carina in the central area and feeble anterior marginal rim.

Description.—Carapace robust and large (540–722 mm long). LV lager than RV. In external view, subtrapezoidal lateral outline: in LV, anterior margin round; posterior margin obtusely angular, forming caudal process; dorsal margin straight and slope to posterior direction; ventral margin slightly curved; in RV, upper half of anterior margin to dorsal margin sinuous. Maximum length across caudal process; maximum height across anterodorsal corner. Anterior and posterior areas flattened. Anterior marginal rim feeble. Surface ornament with three horizontal carinae in central area. Tops of three carinae blunt; middle one blunt and spreads anteriorly like a fan; bottom one finer and pointed posteriorly. Marginal rim developed along anterior margin. In internal view, amphidont-type hingement: in LV, round socket of anterior element; slightly swelling tooth at anterior terminal of median bar; blunt smooth median bar; rectangular socket of posterior element; in RV round node as anterior element; shallow round socket at anterior terminal of median groove, gradually connected to median groove; round tooth as posterior element. Anterior marginal zone width more than 10% of the maximum valve length. Marginal pore canals moderately long. 16 anterior and four posterior pore canals.

Etymology.—Named after the fanlike carina. "*flabelli*" means fan in Latin and "*carinus*" is the masculine singular nominative of "*carina*".

Types.—Holotype: MPC-29116, LV, adult, 342-U1407A-22X-2W, 20–22, Danian. Paratypes: SIO-BIC-C12187, RV, adult, 342-U1407A-22X-4W, 124–126, Danian; MPC-29117, LV, adult, 342-U1407C-17X-5W, 35–37.5, Selandian; SIO-BIC-C12188, LV, adult, 342-U1407A-22X-4W, 124–126, Danian.

Measurement.—Table 1.

Occurrence.—Maastrichtian sediments at ODP Sites 1052 (Majoran, 1999) and 1050 (Guernet and Bellier, 2000), North Atlantic; upper Paleocene to lower Eocene sediments at DSDP Site 401, North Atlantic (Yamaguchi and Norris, 2012); lower to middle Paleocene sediments at IODP Site U1407, North Atlantic (this study).

Remarks.—This new species is similar to *Phacorhabdotus senegalensis* Colin, 1987, originally described from Danian sediments in Senegal and reported as *P.* aff. *sculptilis* from middle Eocene sediments at DSDP Sites 612 and 613, off New Jersey (Cronin and Compton-Gooding, 1987). It is distinguishable from *P. senegalensis* in having a more angular anterodorsal corner, a blunter horizontal carina in the central area, a subtle carina in the posterodorsal area, and a broader flattened ventral area. This new species is different from *Phacorhabdotus* sp. 3 of Guernet and Danelian (2006) in having a blunter carina in the central area and lacking an upward tapering near the posterodorsal corner. *P. flabellicarinus* sp. nov. is similar to *P. anteronudus* Coles and Whatley, 1989 in lateral outline and a thick middle carina, but is distinguished from the latter species by the middle carina being blunter than the bottom carina and spreading out like a fan. *Phacorhabdotus anteronudus* was originally described from lower Oligocene sediments at DSDP Site 549, North Atlantic.

Phacorhabdotus inaequicostata Colin and Donze in Donze *et al*., 1982

Figures 6D, E, 10A, 12A

Phacorhabdotus inaequicostata Colin and Donze in Donze *et al*., 1982, p. 296, pl. 13, fig. 11.

Phacorhabdotus cf. *inaequicostata* Colin and Donze. Majoran *et al*., 1998, p. 68, pl. 2, fig. 12.

Description.—Carapace robust and large (796 μm long). In external view, subtrapezoidal lateral outline: anterior margin round; posterior margin obtusely angular, forming a caudal process; dorsal margin straight and sloping toward posterior; ventral margin slightly curved. Maximum length across caudal process; maximum height across anterodorsal corner. Anterior and posterior areas flattened. Surface ornament with three narrow carinae running horizontally in central area. Tops of three carinae blunt; middle one blunt; bottom one longer that others and pointed posteriorly with short spine. Narrow carina along dorsal margin, extends from anterodorsal corner toward posterodorsal corner. Swelling below bottom horizontal carina. Marginal rim developed along anterior margin. In internal view, lophodont-type hingement: in LV, shallow elongated socket as anterior element, smooth median bar, and shallow wedgelike socket as posterior element. Anterior marginal zone width more than 10% of the maximum valve length. Marginal pore canals long, swelling and curved: 16 anterior and eleven posterior pore canals. Striae on anterior and posterior marginal zones.

*Material.—*MPC-29115, LV, adult, 342-U1407B-19X-3W, 82–84, Maastrichtian.

Measurement.—Table 1.

Occurrence.—The upper Campanian Abiod and Maastrichtian El Haria formations in Tunisia (Donze *et al*., 1982); Maastrichtian sediments at DSDP Site 327, 356, 529 and ODP Site 698, South Atlantic (Majoran *et al*., 1998); Maastrichtian sediments at IODP Site U1407, North Atlantic (this study).

Remarks.—Its outline, three horizontal carinae, broad marginal zone, and the shape of the marginal pore canals indicate affiliation to *Phacorhabdotus*, although the specimen does not possess the amphidont-type hingement that is typical of the genus.

Phacorhabdotus inaequicostata is similar to *P. senegalensis* Colin, 1987 in lateral outline, but is distinguished from the latter taxon by having a slender carapace, a more angular posterior margin, and a shorter middle carina. *Phacorhabdotus inaequicostata* has a height/length (H/L) ratio of 0.49, whereas *P. senegalensis* shows H/L ratios of 0.55–0.61 in the SEM images of Colin (1987). The middle carina of *P. inaequicostata* generates behind the anterodorsal corner. On the other hand, the middle carina of *P. senegalensis* appears just below the corner. *Phacorhabdotus inaequicostata* is similar to *P. anteronudus* Coles and Whatley, 1989 and *P. mazzinireticulatus* Yasuhara, Hunt, Okahashi, and Brandão, 2015 in the lateral outline and the three lateral carinae that are the same thickness, but is different from the latter two species in having the top and middle carinae with the same length. Unlike *P. anteronudus* it is not punctate in the posterior area, nor is that area reticulated as in *P. mazzinireticulatus. Phacorhabdotus mazzinireticulatus* was originally described from modern sediments in the southeastern Pacific.

Genus ***Pterygocythere*** Hill, 1954
Pterygocythere sp.

Figures 6F–J, 10B, 12B

Description.—Juvenile carapace thin and large (812–873 μm long). In external view, lateral outline subtriangular; anterior and posterior margins round; dorsal margin arched and sloping posteriorly; ventral margin sinuous. Maximum length across middle of valve; maximum height across anterodorsal corner. Feeble marginal denticles located at posterior margin. Ventro-central area swollen. Narrow flattened areas along margins. Surface smooth with two ventral carinae. Carina located in ventro-central area and curved concave up; another located on flattened ventral surface. In internal view, lophodont-type hingement: in LV, elongated socket with crenulation as anterior element; smooth median bar; elongated socket with crenulation as posterior element. V-shaped frontal muscle scar. Adductor muscle scars formed by vertical row of four elliptical scars. Anterior marginal zone width less than 10% of the maximum valve length. Twelve short pore canals in anterior marginal zone. Striae in anterior marginal zone.

Material.—MPC-29106, LV, juvenile, 342-U1407C-14X-6W, 21–23, Thanetian; SIO-BIC-C12164, RV, juvenile, 342-U1407C-14X-6W, 21–23, Thanetian; SIO-BIC-C12165, RV, juvenile, 342-U1407B-19X-3W, 22–24, Maastrichtian.

Measurement.—Table 1.

Remarks.—The subtriangular lateral outline, smooth surface, horizontal carina in the ventral area, and a V-shaped frontal scar indicate that the species belongs to the genus *Pterygocythere*. The narrow marginal zone with short marginal pore canals suggests juvenile specimens. Since we have not found adult specimens from the sediment samples, we place the species in open nomenclature.

Genus ***Ryugucivis*** Yasuhara, Hunt, Okahashi, and Brandão, 2015
Ryugucivis blumi sp. nov.

Figures 7A–D, 10C, 12C

Diagnosis.—A *Ryugucivis* species with three blunt carinae and finer reticulation.

Description.—Carapace robust and large (702–863 μm long). In external view, lateral outline rectangular: anterior margin round; posterior margin obtusely tapering at ventral one-third, forming caudal process; dorsal margin slightly sinuous and sloping posteriorly; ventral margin slightly sinuous. Maximum length across caudal process; maximum height across anterodorsal corner. Marginal rims developed along anterior and posterior margins. Marginal denticles located along ventral half of posterior margin. Surface ornamented with reticulation and three horizontal carinae. Reticulation formed by rectangular primary fossae, fine muri, and secondary reticulation. Carinae running horizontally in ventro-central, central, and dorso-central areas: top carina slightly arched and cut off; anterior part of top carina bent like a hook; middle carina blunt, running through subcentral tubercle and is then cut off; bottom carina concave upward. In internal view, amphidont-type hingement; in LV, half round socket as anterior element; smooth median bar that ends anteriorly in round tooth; half round socket as posterior element. Anterior marginal zone width less than 10% of the maximum valve length. Marginal pore canals straight; 15 pore canals in anterior marginal zone; nine pore canals in posterior marginal zone. Striae running in marginal zone.

Etymology.—In honor of Peter Blum (Texas A & M University) who studies petrophysics of deep-sea sediments and rocks and led IODP Exp 342 as Staff Scientist.

Types.—Holotype: MPC-29121, LV, adult, 342-U1407C-18X-3W, 122–124, Selandian. Paratypes: SIO-BIC-C12160, LV, adult, 342-U1407C-20X-4W, 44–46, Danian; SIO-BIC-C12161, LV, adult, 342-U1407C-20X-4W, 49–51, Danian.

Measurement.—Table 1.

Remarks.—*Ryugucivis blumi* sp. nov. is different from *R. jablonskii* Yasuhara, Hunt, Okahashi, and Brandão, 2015, *R. acuminata* Yasuhara, Hunt, Okahashi, and Brandão, 2015, and *R. obtusa* Yasuhara, Hunt, Okahashi, and Brandão, 2015 in having three blunt horizontal carinae and finer reticulation. Those three species were originally described from Cretaceous and Miocene sediments in the Atlantic Ocean.

Ryugucivis sp.

Figures 7E–H, 10D, 12D

Phacorhabdotus? aff. *marssoni* (Bonnema). Swain, 1978, p. 921, pl. 5, figs. 4, 5, pl. 6, figs. 1, 2.
Imhotepia sp. Majoran, 1999, pl. 2, fig. 5.

Description.—Juvenile carapace thin and large (625–834 μm long). In external view, lateral outline subrectangular: anterior margin round; posterior margin tapering, forming a caudal process; dorsal margin straight or slightly sinuous and sloping posteriorly; ventral margin sinuous. Maximum length across caudal process; maximum height across anterodorsal corner. Marginal denticles along anterior margin and ventral half of posterior margin. Anterior marginal rim narrow. Surface ornamentation of primary and secondary reticulation. Primary reticulation framed by rectangular and polygonal fossae. Elongated rectangular fossae in central area; polygonal fossae in anterior area. Distinctive muri running from posterior corner to middle of dorsal margin and curved concave down. Further distinctive muri running horizontally in central area, parallel to anterior margin in anterior area, and along dorsal margin. Six to nine fossae, forming secondary reticulation, framed by fossae of primary reticulation. In internal view, lophodont-type hingement: in LV, arched groove of anterior element; smooth median bar; ovate socket of posterior element. Anterior marginal zone width less than 10% of the maximum valve length. Vestibulum developed in posterior marginal zone. Marginal pore canals straight or bifurcated; eleven pore canals in anterior marginal zone; 13 pore canals in posterior marginal zone. Striae running on marginal zone.

Types.—MPC-29122, LV, juvenile, 342-U1407B-19X-3W, 102–104, Maastrichtian; SIO-BIC-C12189, RV, juvenile, 342-U1407B-19X-3W, 122–124, Maastrichtian; MPC-29123, LV, juvenile, 342-U1407B-19X-3W, 42–44, Maastrichtian; SIO-BIC-C12190, LV, juvenile, 342-U1407B-19X-3W, 82–84, Maastrichtian.

Measurement.—Table 1.

Occurrence.—Upper Campanian sediments at DSDP Site 392, North Atlantic (Swain, 1978); Maastrichtian sediments at ODP Site 1052, North Atlantic (Majoran, 1999); Maastrichtian sediments at IODP Site U1407, North Atlantic (this study).

Remarks.—The outline and costate ornamentation suggest that the species belongs to *Ryugucivis* Yasuhara, Hunt, Okahashi, and Brandão, 2015. Swain (1978) exhibits adult specimens of the species with amphidont-type hingement and a broad anterior marginal zone. Our specimens are juveniles, because they have a narrow anterior marginal zone and lophodont-type hingement. Changes in hingement through ontogeny were reported in some species (Tsukagoshi and Kamiya, 1996). We consider that the species is a new taxon. However, we have not found adult specimens by which to define types. We therefore do not propose a new scientific name for the taxon. The species is similar to *Ambocythere* cf. *ramosa* Bold, 1965 of Guernet and Bellier (2000) in lateral outline and reticulate surface ornamentation but is distinguished from the latter taxon by having a reticulated anterior area and coarser reticulation. This new species is different from *R. obtusa* in having a coarser primary reticulation with larger elongated fossae and feeble secondary reticulation in the anterior area.

Genus ***Trachyleberidea*** Bowen, 1953 emend. Haskins, 1963

Trachyleberidea cronini sp. nov.

Figures 7I, J, 8A–E, 10E, 12E

Trachyleberidea sp. Guernet, 1982, p. 48, pl. 4, figs. 2, 9; Yamaguchi and Norris, 2012, p. 37, fig. 3.21; Bergue *et al*., 2013, p. 29, fig. 2L–M.
Trachyleberidea cf. *cubensis* (Bold). Cronin and Compton-Gooding, 1987, p. 442, pl. 4, fig. 5.
Trachyleberidea pisinensis (Kollmann). Coles, 1996, pl. 2, figs. 11–13; Rodriguez-Lazaro and Garcia-Zaraga, 1996, pl. 1, fig. 16.

Diagnosis.—A *Trachyleberidea* species with blunt marginal rims, coarse reticulation with blunt muri, and distinctive marginal denticles.

Description.—Carapace robust and large (739–867 μm long). In external view, lateral outline subrectangular: anterior margin round; posterior margin tapering; dorsal margin straight or slightly sinuous. Maximum length across the caudal process; maximum height across anterodorsal corner. Marginal denticles developed along anterior margin and ventral half of posterior margin. Distinct spine often projected at caudal process. Anterior marginal rims developed and extended to dorsal and ventral margins. Posterior marginal rim developed. Blunt carina slightly arched along posterior half of dorsal margin and bent like a hook near posterodorsal corner. Surface ornamented with reticulation formed by rectangular and polygonal fossae and blunt muri. Trefoil structure shown in fossae. Sexual dimorphism distinct: male form more elongated than female form; $(L-H)/L$ ratio > 0.5 in male form, < 0.5 in female form. In internal view, amphidont-type hingement: in LV, round socket as anterior element; smooth median bar with node at anterior end; half round socket as posterior element; in RV, rectangular tooth as anterior element; median groove with round socket at anterior end, gradually connected to groove; rectangular tooth as posterior element. Anterior marginal zone width more than 10% of the maximum valve length. Anterior marginal pore canals often straight, medianly swelling, and bifurcated. Sixteen pore canals in anterior marginal zone. Posterior marginal pore canals short and blunt. Six pore canals in posterior marginal zone. Striae in anterior marginal zone.

Etymology.—In honor of Thomas M. Cronin (U.S. Geological Survey, Reston, Virginia), who studies deep-sea ostracodes.

Types.—Holotype: MPC-29124, LV, adult, female, 342-U1407C-20X-5W, 34–36, Danian. Paratypes: SIO-BIC-C12166, RV, adult, male, 342-U1407C-17X-2W, 114–116, Selandian; SIO-BIC-C12167, LV, adult, female, 342-U1407A-21X-3W, 20–22, Selandian; MPC-29125, RV, adult, male, 342-U1407C-17X-4W, 68–70, Selandian.

Other examined materials.—Four adult specimens from U1407 and 17 adult specimens from DSDP Site 401.

Measurement.— Figure 14, Table 1.

Occurrence.—Lower to middle Eocene sediments at DSDP Site 390 (Guernet, 1982); lower to middle Eocene sediments at DSDP Sites 612 and 613, North Atlantic (Cronin and Compton-Gooding, 1987); lower Paleocene to upper Oligocene sediments at DSDP Sites 549 and 550, North Atlantic (Coles, 1996); lower to middle Eocene sediments in the Basque Basin, Spain (Rodriguez-Lazaro and Garcia-Zaraga, 1996); upper Paleocene to lower Eocene sediments at DSDP Site 401, North Atlantic (Yamaguchi and Norris, 2012); upper Eocene to lower Oligocene sediments at DSDP Site 515, South Atlantic (Bergue *et al*., 2013); lower to middle Paleocene sediments at IODP Site U1407, North Atlantic (this study).

Remarks.—*Trachyleberidea cronini* sp. nov. is similar to *T. elegans* Guernet, 1985, originally described from Eocene to Oligocene sediments at DSDP Site 214, Indian Ocean, in lateral outline and marginal rims but is distinguished from the latter species by having blunter dorsal and ventral carinae extending from the anterior marginal rim, coarser reticulation with blunter muri and fewer fossae, and a subtle subcentral tubercle. The new species is different from *T. pisinensis* (Kollmann, 1962) in having a larger carapace with reticulation with more fossae (Yamaguchi and Norris, 2012). *Trachyleberidea cronini* sp. nov. is distinguished from *T. cubensis* (Bold, 1946), originally described from the Eocene of Cuba, by having a coarser reticulation with fewer fossae and lacking fossae before the anterior marginal rim. Bergue *et al*. (2013) considered that the new species is congeneric to *Trachyleberidea* sp. of Guernet and Fourcade (1988) from Oligocene to Pliocene sediments at DSDP Site 612. However, *T. cronini* sp. nov. is different from the latter species in having coarser reticulation with fewer fossae and blunt muri.

Family Xestoleberididae Sars, 1928

Genus ***Platyleberis*** Bonaduce and Danielopol, 1988

Platyleberis sp.

Figures 8F, G, 10F

Platyleberis chamela (Bold). Rodriguez-Lazaro and Garcia-Zaraga, 1996, pl. 1, fig. 8.

Platyleberis sp. Yamaguchi and Norris, 2012, p. 36, figs. 3.18, 3.19.

Material.—MPC-29118, LV, adult, 342-U1407C-17X-4W, 68–70, Selandian; SIO-BIC-C12172, RV, adult, 342-U1407C-18X-3W, 15–17, Selandian.

Measurement.—Table 1.

Occurrence.—Upper Paleocene to middle Eocene sediments in the Basque Basin, Spain (Rodriguez-Lazaro and Garcia-Zaraga, 1996); upper Paleocene to early Eocene sediments at DSDP Site 401, North Atlantic (Yamaguchi and Norris, 2012); middle Paleocene sediments at IODP Site U1407, North Atlantic (this study).

Remarks.—The specimens are different from *Platyleberis chamela* (Bold, 1960) in having the anterodorsal corner as high as the posterodorsal corner. In *P. chamela* the anterodorsal corner is lower than the posterodorsal corner. They are similar to *Xestoleberis oppoae* Yasuhara, Okahashi, and Cronin, 2009b in lateral outline but differ from the latter taxon in having a smooth surface without plications in the central area in external view and a marginal zone with a narrower vestibulum in internal view. *Xestoleberis oppoae* was originally described from Quaternary sediments from ODP Site 1055, North Atlantic.

Acknowledgements

This research used samples provided by the Integrated Ocean Drilling Program. We are grateful to Megumi Saito-Kato (NMNS) and Harim Cha (SIO) for helping to register and deposit the specimens. We thank Michael Schudack (Freie Universität, Berlin) and Alan Lord (Senckenberg Research Institute and Natural History Museum, Frankfurt) for their kind help in collecting literature, and Gene Hunt (Smithsonian Institution National Museum of Natural History, Washington, D.C.) for his views about the taxonomy of *Poseidonamicus*. We would also like to express our thanks to Moriaki Yasuhara (University of Hong Kong) for his critical review and help in collecting literature, and Yasunari Shigeta (National Museum of Nature and Science, Tsukuba) and an anonymous reviewer for their critical reviews and useful comments. This study was financially supported by IODP Exp 342 After Cruise Research Program of Japan Agency for Marine-Earth Science and Technology.

References

Alvarez Zarikian, C. A., 2015: Cenozoic bathyal and abyssal ostracodes beneath the oligotrophic South Pacific Gyre (IODP Expedition 329 Sites U1367, U1368 and U1370). *Palaeogeography, Palaeoclimatology, Palaeoecology*, vol. 419, p. 115–142.

Athersuch, J., Horne, D. J. and Whittaker, J. E., 1989: *Marine and Brackish Water Ostracoda (Superfamilies Cypridacea and Cytheracea: Keys and Notes for the Identification of the Species)*, 343 p. Linnean Society of London and the Estuary and Brackish-water Sciences Association, London.

Ayress, M., Barrows, T., Passlow, V. and Whatley, R., 1999: Neogene to Recent species of *Krithe* (Crustacea: Ostracoda) from the Tasman Sea and off southern Australia with description of five new species. *Records of the Australian Museum*, vol. 51, p. 1–22.

Benson, R. H., 1971: A new Cenozoic deep-sea genus, *Abyssocythere* (Crustacea: Ostracoda: Trachyleberididae), with descriptions of five new species. *Smithsonian Contributions to Paleobiology*, vol. 7, p. 1–25.

Benson, R. H., 1972: The *Bradleya* problem, with description of two new psychrospheric ostracode genera, *Agrenocythere* and *Poseidonamicus* (Ostracoda: Crustacea). *Smithsonian Contributions to Paleobiology*, vol. 12, p. 1–138.

Bergue, C. T., 2006: A aplicação dos ostracodes (Crustacea) em pesquisas paleoceanográficas e paleoclimáticas. *Terræ Didatica*, vol. 2, p. 54–66.

Bergue, C. T. and Coimbra, J. C., 2008: Abordagens faunísticas e geoquímicas em microfósseis calcários e suas aplicações à paleoceanografia e paleoclimatologia. *Boletim do Museu Paraense Emílio Goeldi. Ciências Naturais*, *Belém*, vol. 3, p. 115–126.

Bergue, C. T., Costa, K. B., Dwyer, G. and Moura, C. V., 2006: Bathyal ostracode diversity in the Santos Basin, Brazilian Southeast Margin: Response to Late Quaternary climate changes. *Revista Brasileira de Paleontologia*, vol. 9, p. 201–210.

Bergue, C. T., Nicolaidis, D. D. and Andrade, K. N., 2013: The Lower Eocene–Lower Oligocene ostracodes from DSDP Site 515B, Brazil Basin, southwestern Atlantic Ocean. *Revista Brasileira de Paleontologia*, vol. 16, p. 27–38.

Bold, W. A. van den, 1946: *Contribution to the Study of Ostracoda with Special Reference to the Tertiary and Cretaceous Microfauna of the Caribbean Region*, 167 p. De Bussy, Amsterdam.

Bold, W. A. van den, 1957: Ostracoda from the Paleocene of Trinidad. *Micropaleontology*, vol. 3, p. 1–18.

Bold, W. A. van den, 1960: Eocene and Oligocene Ostracoda of Trinidad. *Micropaleontology*, vol. 6, p. 391–418.

Bold, W. A. van den, 1965: New species of the ostracod genus *Ambocythere*. *Annals and Magazine of Natural History*, vol. 8, p. 1–18.

Bonaduce, G. and Danielopol, D. L., 1988: To see and not to be seen: the evolutionary problems of the Ostracoda Xestoleberididae. *In*, Hanai, T., Ikeya, N. and Ishizaki, K. *eds*., *Evolutionary Biology of Ostracoda*, p. 375–398. Kodansha, Tokyo and Elsevier, Amsterdam.

Bowen, R. N. C., 1953: Ostracoda from the London Clay. *Proceedings of the Geologists' Association*, vol. 64, p. 276–292.

Brady, G. S., 1868: A monograph of the recent British Ostracoda. *Transactions of the Linnean Society*, vol. 26, p. 353–495.

Brady, G. S., 1880: Report on the Ostracoda dredged by H.M.S. Challenger during the years 1873–1876. *Report on the Scientific Results of the Voyage of H.M.S. Challenger during the Years 1873–76, Zoology*, vol. 1, p. 1–184.

Brady, G. S., Crosskey, H. W. and Robertson, D., 1874: A monograph of the post-Tertiary Entomostraca of Scotland including species from England and Ireland. *Palaeontographical Society*, vol. 28, p. 1–274.

Brandão, S. N., Angel, M. V., Karanovic, I., Parker, A., Perrier, V., Sames, B. and Yasuhara, M., 2016: *World Ostracoda Database* [online]. [Cited 31 January 2016]. Available from http://www.marinespecies.org/ostracoda.

Brökeland, W. and George, K. H., 2009: Editorial: Deep-sea taxonomy—a contribution to our knowledge of biodiversity. *Zootaxa*, vol. 2096, p. 6–8.

Bubikyan, S. A., 1958: Ostracoda from Paleogene deposits of the Erevan Basin. *Izvestiya Akademii Nauk Armyanskoy SSR*, *Seriya Geologiya-Geografiya*, vol. 11, p. 3–16. (*in Russian; original title translated*)

Burnett, J. A., 1998: Upper Cretaceous. *In*, Bown, P. R. *ed*., *Calcareous Nannofossil Biostratigraphy*, p. 133–199. Kluwer Academic Publishers, Dordrecht.

Coles, G., 1996: A preliminary ostracod zonation for the Cenozoic deep water North Atlantic. *Proceedings of 2nd European Ostracodologists Meeting*, *Glasgow 1993*, p. 86–92.

Coles, G. and Whatley, R. C., 1989: New Palaeocene to Miocene genera and species of Ostracoda from DSDP sites in the North Atlantic. *Revista Española de Micropaleontología*, vol. 21, p. 81–124.

Coles, G. P., Whatley, R. C. and Moguilevsky, A., 1994: The ostracod genus *Krithe* from the Tertiary and Quaternary of the North Atlantic. *Palaeontology*, vol. 37, p. 71–120.

Colin, J.-P., 1987: Étude systématique des ostracodes de la Formation des Madeleines (Danien du Sénégal). *Cahiers de Micropaléontologie*, *Nouvelle Série*, vol. 2, p. 113–124.

Cronin, T. M. and Compton-Gooding, E. E., 1987: Cenozoic Ostracoda from Deep Sea Drilling Project Leg 95 off New Jersey (Sites 612 and 613). *In*, Poag, C. W., Watts, A. B. *et al. eds*., *Initial Reports of the Deep Sea Drilling Project*, vol. 95, p. 439–449. U.S. Government Printing Office, Washington, DC.

DeNinno, L. H., Cronin, T. M., Rodriguez-Lazaro, J. and Brenner, A., 2015: An early to mid-Pleistocene deep Arctic Ocean ostracode fauna with North Atlantic affinities. *Palaeogeography*, *Palaeoclimatology*, *Palaeoecology*, vol. 419, p. 90–99.

Donze, P., Colin, J.-P., Damotte, R., Oertli, H. J., Peypouquet, J.-P. and Said, R., 1982: Les Ostracodes du Campanien terminal à l'Éocène inférieur de la coupe du Kef, Tunisie nord-occidentale. *Bulletin des Centres de Recherches Exploration-Production Elf-Aquitaine*, vol. 6, p. 273–335.

Expedition 342 Scientists, 2012: Paleogene Newfoundland sediment drifts. *Integrated Ocean Drilling Program Preliminary Report*, vol. 342, doi: 10.2204/iodp.pr.342.2012.

Gradstein, F. M., Ogg, J. G., Schmitz, M. D. and Ogg, G. M., 2012: *The Geological Time Scale 2012*, 1176 p. Elsevier, Boston.

Gründel, J., 1973: Zur Entwicklung der Trachyleberididae (Ostracoda) in der Unterkreide und in der tieferen Oberkreide. Teil I: Taxonomie. *Zeitschrift für Geologische Wissenschaften*, vol. 1, p. 1463–1474.

Guernet, C., 1982: Contribution à l'étude des faunes abyssales: les Ostracodes paléogènes du Bassins des Bahamas, Atlantique Nord (D.S.D.P., Leg. 44). *Revue de Micropaléontologie*, vol. 25, p. 40–56.

Guernet, C., 1985: Ostracodes paléogènes de quelques sites 'D.S.D.P.' de l'Océan Indien (Legs 22 et 23). *Revue de Paléobiologie*, vol. 4, p. 279–295.

Guernet, C. and Bellier, J.-P., 2000: Ostracodes paléocènes et éocènes du Blake Nose (Leg ODP 171B) et évolution des envrionments bathyaux au large de la Floride. *Revue de Micropaléontologie*, vol. 43, p. 249–279.

Guernet, C. and Danelian, T., 2006: Ostracodes bathyaux du Crétacé terminal–Éocène moyen en Atlantique tropical (Plateau de Demer-

ara, Leg 207). *Revue de Micropaléontologie*, vol. 49, p. 215–225.
Guernet, C. and Fourcade, E., 1988: Cenozoic ostracodes from Hole 628A, ODP Leg101, Bahamas. *In*, Austin, J. A., Jr., Schlager, W. *et al*. *eds*., *Proceedings of the Ocean Drilling Program*, *Scientific Results*, vol. 101, p. 139–151. Ocean Drilling Program, College Station.
Haskins, C. W., 1963: Revision of the ostracode genus *Trachyleberidea* Bowen. *Micropaleontology*, vol. 9, p. 71–74.
Hazel, J. E., 1967: Classification and distribution of the Recent Hemicytheridae and Trachyleberididae (Ostracoda) off Northeastern North America. *U. S. Geological Survey Professional Paper*, vol. 564, p. 1–49.
Hill, B. L., 1954: Reclassification of winged *Cythereis* and winged *Brachycythere*. *Journal of Paleontology*, vol. 28, p. 804–826.
Horne, D. J., Cohen, A. and Martens, K., 2002: Taxonomy, morphology and biology of Quaternary and living Ostracoda. *In*, Holmes, J. A. and Chivas, A. R. *eds*., *The Ostracoda: Appications in Quaternary Research*, p. 5–36. American Geophysical Union, Washington, DC.
Howe, H. V. and Laurencich, L., 1958: *Introduction to the Study of Cretaceous Ostracoda*, 536 p. Louisiana State University, Baton Rouge.
Hunt, G., 2007: Morphology, ontogeny, and phylogenetics of the genus *Poseidonamicus* (Ostracoda: Thaerocytherinae). *Journal of Paleontology*, vol. 81, p. 607–631.
Kollmann, K., 1962: Ostracoden aus dem mitteleozänen "Flysch" des Beckens von Pazin (Istrien, Jugosiawien). *Verhandlungen der Geologischen Bundesanstalt*, vol. 1962, p. 187–227.
Majoran, S., 1999: Palaeoenvironment of Maastrichtian ostracods from ODP Holes 1049B, 1050C and 1052E in the Western North Atlantic. *Journal of Micropalaeontology*, vol. 18, p. 125–136.
Majoran, S., Kucera, M. and Widmark, J. G. V., 1998: Maastrichtian deep-sea ostracods from DSDP/ODP Sites 327, 356, 527, 528, 529 and 698 in the South Atlantic. *Revista Española de Micropaleontología*, vol. 30, p. 59–73.
Martínez-García, B., Rodríguez-Lázaro, J., Pascual, A. and Mendicoa, J., 2015: The "Northern guests" and other palaeoclimatic ostracod proxies in the late Quaternary of the Basque Basin (S Bay of Biscay). *Palaeogeography*, *Palaeoclimatology*, *Palaeoecology*, vol. 419, p. 100–114.
Martini, E., 1971: Standard Tertiary and Quaternary calcareous nannoplankton zonation. *In*, Farinacci, A. *ed.*, *Proceedings of Second Planktonic Conference*, *Roma 1970*, p. 739–785. Edizioni Tecnoscienza, Roma.
Mazzini, I., 2005: Taxonomy, biogeography and ecology of Quaternary benthic Ostracoda (Crustacea) from circumpolar deep water of the Emerald Basin (Southern Ocean) and the S Tasman Rise (Tasman Sea). *Senckenbergiana Maritima*, vol. 35, p. 1–119.
Norris, R. D., Wilson, P. A., Blum, P. and the Expedition 342 Scientists, 2014: Paleogene Newfoundland sediment drifts and MDHDS Test. *Proceedings of the Integrated Ocean Drilling Program*, vol. 342, doi: 10.2204/iodp.proc.342.2014.
Ozawa, H., 2013: The history of sexual dimorphism in Ostracoda (Arthropoda, Crustacea) since the Palaeozoic. *In*, Moriyama, H. *ed.*, *Sexual Dimorphism*, p. 51–80. InTech Open Access Company, Rijeka.
Puri, P. S., 1953: Contribution to the study of the Miocene of the Florida Panhandle. *Florida Geological Survey*, *Geological Bulletin*, vol. 36, p. 217–309.
R Core Team, 2015: R: A language and environment for statistical computing. R Foundation for Statistical Computing, Vienna. https://www.R-project.org/.
Rodriguez-Lazaro, J. and Garcia-Zaraga, E., 1996: Paleogene deep-marine ostracodes from the Basque Basin. *Proceedings of 2nd European Ostracodologists Meeting*, *Glasgow 1993*, p. 79–86.
Sanfilippo, A. and Nigrini, C., 1998: Code numbers for Cenozoic low latitude radiolarian biostratigraphic zones and GPTS conversion tables. *Marine Micropaleontology*, vol. 33, p. 109–117 and p. 121–156.
Sars, G. O., 1928: Ostracoda, parts 15 and 16. *An Account of the Crustacea of Norway with Short Description and Figures of All the Species*, vol. 9, p. 241–277.
Silverman, B. W., 1986: *Density Estimation for Statistics and Data Analysis*, 176 p. Chapman and Hall, London.
Swain, F. M., 1978: Notes on Cretaceous Ostracoda from DSDP Leg 44, Sites 390 and 392. *In*, Benson, W. E., Sheridan, R. E. *et al. eds*., *Initial Reports of the Deep Sea Drilling Project*, vol. 44, p. 921–937. U.S. Government Printing Office, Washington, DC.
Sylvester-Bradley, P. C., 1948: The ostracode genus *Cythereis*. *Journal of Paleontology*, vol. 22, p. 792–797.
Sylvester-Bradley, P. C. and Benson, R. H., 1971: Terminology for surface features in ornate ostracodes. *Lethaia*, vol. 4, p. 249–286.
Tsukagoshi, A. and Kamiya, T., 1996: Heterochrony of the ostracod hingement and its significance for taxonomy. *Biological Journal of the Linnean Society*, vol. 57, p. 343–370.
Wade, B. S., Pearson, P. N., Berggren, W. A. and Pälike, H., 2011: Review and revision of Cenozoic tropical planktonic foraminiferal biostratigraphy and calibration to the geomagnetic polarity and astronomical time scale. *Earth Science Reviews*, vol. 104, p. 111–142.
Whatley, R. and Coles, G., 1987: The late Miocene to Quaternary Ostracoda of Leg 94, Deep Sea Drilling Project. *Revista Española de Micropaleontología*, vol. 19, p. 33–97.
Whatley, R. C. and Dingle, R. V., 1989: First record of an extant, sighted shallow-water species of the genus *Poseidonamicus* Benson (Ostracoda) from the continental margin of south-western Africa. *Annals of the South African Museum*, vol. 98, p. 437–457.
Whatley, R. C., Downing, S. E., Kesler, K. and Harlow, C. J., 1986: The ostracod genus *Poseidonamicus* from the Cainozoic of D.S.D.P. sites in the S.W. Pacific. *Revista Española de Micropaleontología*, vol. 18, p. 387–400.
Yamaguchi, T., Matsui, H. and Nishi, H., 2017: Taxonomy of Maastrichtian–Thanetian deep-sea ostracodes from U1407, IODP Exp 342, off Newfoundland, Northwestern Atlantic, part 1: Families Cytherellidae, Bairdiidae, Pontocyprididae, Bythocytheridae, and Cytheruridae. *Paleontological Research*, vol. 21, p. 54–75.
Yamaguchi, T. and Norris, R. D., 2012: Deep-sea ostracode turnovers through the Paleocene–Eocene thermal maximum in DSDP Site 401, Bay of Biscay, North Atlantic. *Marine Micropaleontology*, vols. 86–87, p. 32–44.
Yamaguchi, T., Norris, R. D. and Bornemann, A., 2012: Dwarfing of ostracodes during the Paleocene–Eocene Thermal Maximum at DSDP Site 401 (Bay of Biscay, North Atlantic) and its implication for changes in organic carbon cycle in deep-sea benthic ecosystem. *Palaeogeography*, *Palaeoclimatology*, *Palaeoecology*, vols. 346–347, p. 130–144.
Yasuhara, M., Grimm, M., Brandão, S. N., Jöst, A., Okahashi, H., Iwatani, H., Ostmann, A. and Martínez Arbizu, P., 2014: Deep benthic ostracodes from multiple core and epibenthic sledge samples in Icelandic waters. *Polish Polar Research*, vol. 35, p. 341–360.
Yasuhara, M., Hunt, G., Cronin, T. M. and Okahashi, H., 2009a: Temporal latitudinal-gradient dynamics and tropical instability of deep-sea species diversity. *Proceedings of National Academy of Science*, vol. 106, p. 21717–21720.
Yasuhara, M., Hunt, G., Okahashi, H. and Brandão, S. N., 2015: Taxonomy of deep-sea trachyleberidid, thaerocytherid, and hemi-

cytherid genera (Ostracoda). *Smithsonian Contributions to Paleobiology*, vol. 96, p. 1–216.
Yasuhara, M., Okahashi, H. and Cronin, T. M., 2009b: Taxonomy of Quaternary deep-sea ostracods from the western north Atlantic Ocean. *Palaeontology*, vol. 52, p. 879–931.

Appendix A. Characters and character states of *Poseidonamicus norrisi* sp. nov. The characters were designed by Hunt (2007).

Character	Character status	
2	Inner lamella width (Adult)	0. relatively narrow
12	C3 fossae	0. undivided
13	Relative position of A1 and B1 fossae	1. B1 nearly ventral to A1
14	Position of A6 fossae	1. dorsal to both M6 and A5
15	Position of D7 fossae	1. D7 positioned relatively dorsal to D6
16	Relative position of B2, B3, and C4 fossae	0. C4 markedly posterior of line between B2 and B3
17	Position of C6D6 mura, relative to C5D5 mura	1. no offset
20	Position of B3, relative to C2 and C3 (Adult)	0. B3 located anterior to C2 and C3
21	Number of AR fossae (Adult)	0. six in LV, six in RV
22	Shape of anterior field fossae	0. fossae distinctly round
23	Anterior field reticulation (Adult)	0. primary reticulation only
24	Posterior field reticulation (Adult)	0. primary only
27	Dorsal ridge above mural loop (Adult)	1. DR continuous above mural loop
28	Dorsal ridge posterior termination (Adult)	1. DR terminates in broad mura extending markedly posterior to D7 fossae
29	Continuity of the posterior dorsal ridge (Adult)	0. DR continuous over ABCD fossae columns
30	Posterior margin denticles	1. denticles connected by a thin sheet of shell material
34	Ocular ridge	0. absent
36	Fovelate reticulum	0. absent
37	Slope of anterior margin rim	1. AMR flat and parallel to commissure
39	Shape of the anterior margin (LV)	0. smoothly curved
40	Anterior cardinal angle (Adult, LV)	0. subdued to moderately prominent hinge ear
41	Shape of posterior margin in lateral view (Adult)	0. slightly caudate/subquadrate
42	Shape of posterior region in dorsal view (Adult)	1. posterior region narrows immediately anterior to PMR, then increases in width